

CIPOS™ Maxi IPM

IM828 Series application note

About this document

Scope and purpose

The scope of this application note is to describe the IM828 product group of CIPOS™ Maxi family and the basic requirements for operating the products in a recommended mode. This is related to the integrated components, such as SiC MOSFET or gate driver IC, as well as to the design of the necessary external circuitry, such as bootstrap or interfacing.

Intended audience

Power electronics engineers who want to design reliable and efficient CIPOS™ Maxi IPM applications.

Table of contents

About this document.....	1
Table of contents.....	1
1 Scope.....	4
1.1 Product line-up.....	4
1.2 Nomenclature.....	4
2 Internal components and package technology	5
2.1 1200 V CoolSiC™ MOSFET	5
2.2 Control IC - 1200 V 6-channel gate driver IC	5
2.3 Thermistor	5
2.4 Package technology	6
3 Product overview.....	7
3.1 Internal circuit and features	7
3.2 Maximum electrical ratings.....	8
3.3 Electrical characteristics.....	9
3.3.1 Statics characteristics.....	9
3.3.1.1 Blocking capability.....	9
3.3.1.2 Output characteristics	9
3.3.1.3 On-state resistance RDS(on) vs. junction temperature TJ	10
3.3.1.4 3 rd quadrant operating mode	10
3.3.2 Dynamic characteristics.....	12
3.3.2.1 Switching characteristics.....	12
3.3.2.2 Body diode reverse recovery characteristics	15
3.3.2.3 SCSOA(short-circuit safe operation area) characteristics.....	16
3.4 Description of the input and output pins	17
3.5 Outline drawing.....	20
4 Interface circuit and layout guide	21
4.1 Input signal connection	21
4.2 Internal deadtime.....	22
4.3 Cross-conduction prevention circuitry.....	22
4.4 Advanced input filter.....	23

4.5	Matched propagation delay	24
4.6	General interface circuit example	25
4.7	Recommended rated output current of power supply	26
4.8	Recommended layout pattern	27
4.8.1	OCP & SCP function	27
4.8.2	Power line	27
4.9	Recommended wiring of shunt resistor and snubber capacitor	29
4.10	Pin and screw hole coordinates for IM828 footprint	30
5	Protection features	31
5.1	Undervoltage protection	31
5.2	Overcurrent protection	32
5.2.1	Timing chart of overcurrent (OC) protection	32
5.2.2	Selecting current sensing shunt resistor	33
5.2.3	Delay time	34
5.3	RFE circuit	34
5.4	Sleep function	36
5.5	Temperature monitor and thermal protection	37
6	Bootstrap circuit	39
6.1	Bootstrap circuit operation	39
6.2	Internal bootstrap functionality characteristics	39
6.3	Initial charging of bootstrap capacitor	40
6.4	Bootstrap supply circuit current at switching mode	41
6.5	Bootstrap circuit design	41
6.5.1	Bootstrap capacitor	41
6.5.2	Bootstrap voltage variance under inverter operating conditions	42
7	Thermal system design	43
7.1	Introduction	43
7.2	Power loss	44
7.2.1	Conduction losses	44
7.2.2	Switching losses	45
7.3	Thermal impedance	45
7.4	Temperature rise considerations and calculation example	46
7.5	Heat sink selection guide	47
7.5.1	Required heat sink performance	47
7.5.2	Heat sink characteristics	47
7.5.2.1	Heat transfer from heat source to heat sink	48
7.5.2.2	Heat transfer within the heat sink	48
7.5.2.3	Heat transfer from heat sink surface to ambient	48
7.5.3	Selecting a heat sink	50
8	Heat sink mounting and handling guidelines	51
8.1	Electrical spacing	51
8.2	Heat sink mounting	52
8.2.1	General guidelines	52
8.2.1.1	Recommended tightening torque	52
8.2.1.2	Screw-tightening to heat sink	54
8.2.1.3	Mounting screw	55
8.2.2	Recommended heat sink shape and mechanical assembly	55
8.3	Handling guidelines	56
8.4	Storage guidelines	56
8.4.1	Recommended storage conditions	56



9 References57

Scope

1 Scope

The scope of this application note is to describe the product group of IM828 and the basic requirements for operating the products in a recommended mode. This is related to the integrated components, such as silicon carbide (SiC) MOSFET or gate driver ICs, as well as to the design of the necessary external circuitry, such as bootstrap or interfacing. Integrating discrete power semiconductors and gate driver ICs into one package allows design engineers to reduce the time and effort spent on design. To meet the strong demand for small size and higher power density, Infineon Technologies has developed a new family of highly integrated intelligent power modules that contain nearly all of the semiconductor components required to drive electronically controlled variable-speed electric motors. They incorporate a three-phase inverter power stage with an SOI gate driver and Infineon's leading-edge CoolSiC™ 1200V Power MOSFETs.

The application note concerns the following products:

IM828-XCC

M828 is a product group of CIPOS™ Maxi IPM family, which are designed for motor drives in commercial applications, such as fan drives, active harmonic filters, PWM rectifiers, and compressor drives for HVAC (heating, ventilating, and air-conditioning) systems, low power general purpose drives (GPD), and pumps applications as well.

1.1 Product line-up

Table 1 Line-up of IM828 product

Part Number	Rating		Topologies	Package	Isolation voltage [Vrms]	Main applications
	Current [A]	Voltage [V]				
IM828-XCC	20	1200	3 ϕ bridge open source	Fully molded dual In-line(DIL) module with direct copper bond(DCB) substrate	2500 Vrms/60 Hz (sinusoidal, 1 min. All pins shorted – heat sink)	PWM rectifier for HVAC, motor drives, fans, and pumps

1.2 Nomenclature

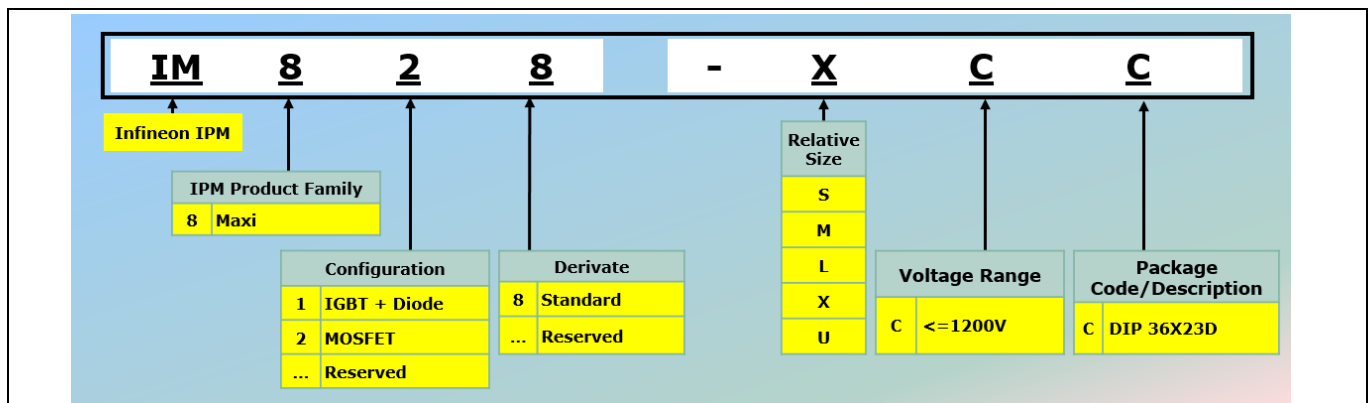


Figure 1 IM828 product group nomenclature

2 Internal components and package technology

2.1 1200 V CoolSiC™ MOSFET

Infineon Technologies introduced 1200 V CoolSiC™ SiC MOSFET technology in 2017^[1]. Silicon carbide (SiC) opens up new degrees of flexibility for designers to harness never before seen levels of efficiency and reliability. In comparison to traditional silicon (Si) based high voltage (> 600 V) switches like IGBTs and MOSFETs, the SiC MOSFET offers a series of advantages. These include the lowest gate charge and device capacitance levels seen in 1200 V switches, less reverse recovery losses of the body diode, temperature-independent low switching losses, and threshold-free on-state characteristics. Infineon's unique 1200 V SiC MOSFET adds additional advantages. Superior gate oxide reliability enabled by state-of-the-art trench design, best-in-class switching and conduction losses, highest transconductance level (gain), threshold voltage of $V_{th,typ} = 4\text{ V}$ and short-circuit robustness. Delivering the highest level efficiency at switching frequencies unreachable by Si-based switches allow for system size reduction, power density increases and high lifetime reliability.

2.2 Control IC - 1200 V 6-channel gate driver IC

The basic feature of this technology is the separation of the active silicon from the base material by means of a buried silicon oxide layer. The buried silicon oxide provides an insulation barrier between the active layer and silicon substrate, and hence reduces the parasitic capacitance tremendously. Moreover, this insulation barrier disables leakage or latch-up currents between adjacent devices. This also prevents the latch-up effect even in case of high dv/dt switching under elevated temperature, and hence provides improved robustness. Besides the thin-film SOI technology provides additional benefits like lower power consumption and higher immunity to radioactive radiation or cosmic rays.^[3] A monolithic single control IC for all 6 MOSFETs provides further advantages, such as bootstrap circuitry, matched propagation delay times, built-in deadtime, anti cross conduction, and all 6 MOSFETs turn-off under fault situations like undervoltage lockout or overcurrent.

2.3 Thermistor

In IM828, the thermistor is integrated in the internal PCB. It is connected between the VTH and VSS pins. A circuit proposal using the thermistor for over-temperature protection is discussed in Section 5.5.

Table 1 Raw data on the thermistor used in IM828

T [°C]	R _{min} [kΩ]	R _{typ} [kΩ]	R _{max} [kΩ]	Tol [%]	T [°C]	R _{min} [kΩ]	R _{typ} [kΩ]	R _{max} [kΩ]	Tol [%]
-40	2662.292	2962.540	3262.789	10.1	45	34.520	36.508	38.496	5.4
-35	1925.308	2133.692	2342.076	9.8	50	28.400	29.972	31.545	5.2
-30	1407.191	1553.414	1699.637	9.4	55	23.485	24.735	25.985	5.1
-25	1038.949	1142.63	1246.312	9.1	60	19.517	20.515	21.514	4.9
-20	774.497	848.747	922.997	8.7	65	16.296	17.097	17.898	4.7
-15	582.690	636.369	690.048	8.4	70	13.670	14.315	14.960	4.5
-10	442.252	481.410	520.568	8.1	75	11.517	12.039	12.561	4.3
-5	338.491	367.303	396.114	7.8	80	9.745	10.169	10.593	4.2
0	261.164	282.537	303.910	7.6	85	8.279	8.625	8.971	4.0
5	203.056	219.036	235.016	7.3	90	7.062	7.345	7.628	3.9
10	159.044	171.081	183.118	7.0	95	6.046	6.279	6.511	3.7
15	125.454	134.586	143.717	6.8	100	5.199	5.388	5.576	3.5
20	99.630	106.605	113.580	6.5	105	4.468	4.640	4.811	3.7

25	79.638	85.000	90.362	6.3	110	3.856	4.009	4.163	3.8
30	64.055	68.203	72.352	6.1	115	3.338	3.477	3.615	4.0
35	51.831	55.059	58.287	5.9	120	2.900	3.024	3.149	4.1
40	42.182	44.708	47.235	5.7	125	2.527	2.639	2.751	4.2

2.4 Package technology

The IM828 series offers the smallest size while providing high power density up to 1200 V, 45 mΩ by employing CoolSiC™ MOSFETs with 6-channel gate driver ICs. It contains all the power components such as the SiC MOSFETs and isolates them from each other and from the heat sink. All low power components such as the gate driver IC and thermistor are assembled on a PCB.

The electric insulation is provided by the DCB itself, which is simultaneously the thermal contact to the heat sink. In order to further decrease the thermal impedance, the internal lead frame design is optimized ^[4]. Figure 2 shows the external view and internal structure of the IM828 package.

The two dummy pins on the package side which fix the inner PCB, have no connection with the internal circuit, which means that the dummy pins have no electrical function and are isolated in the package.

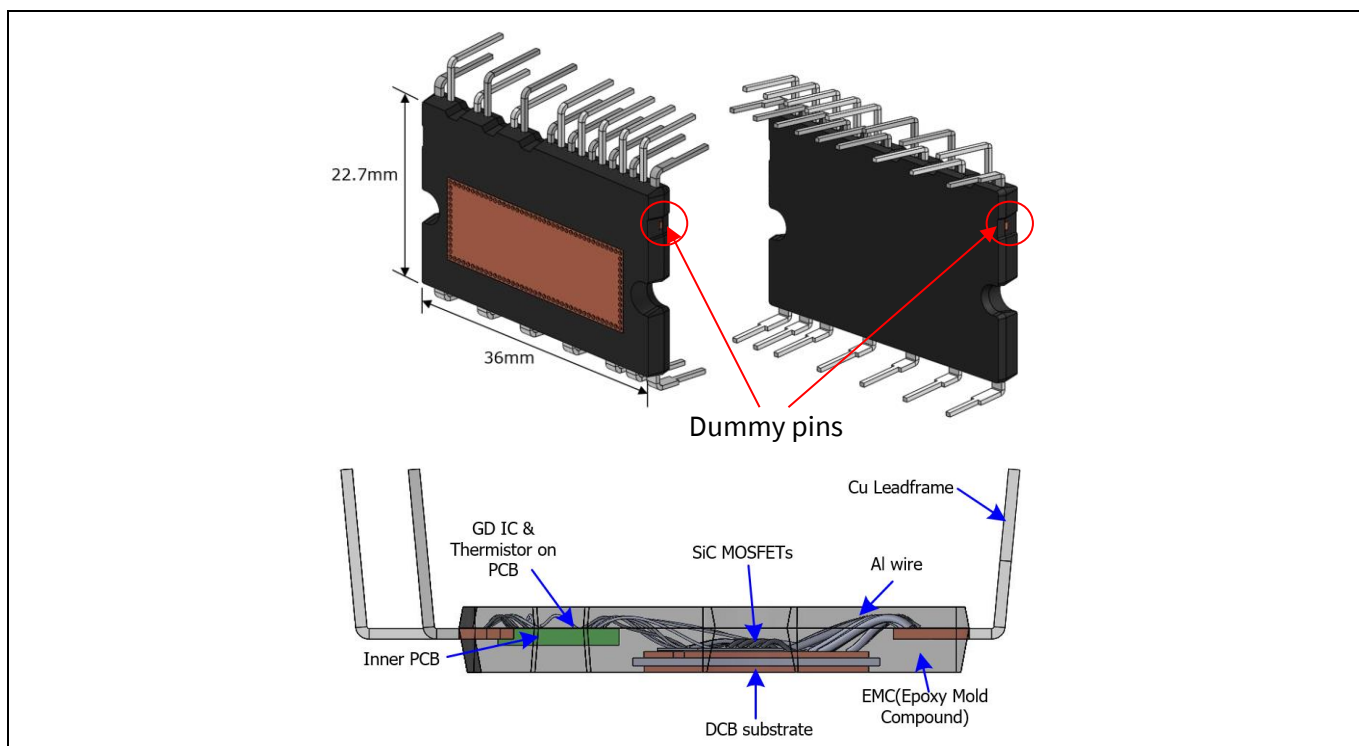


Figure 2 External view and internal structure of CIPOS™ Maxi package (DIP 36x23D)

3 Product overview

3.1 Internal circuit and features

Figure 3 illustrates the internal block diagram of the IM828. It consists of a three-phase inverter circuit and a gate driver IC with control functions. The detailed features and integrated functions of IM828 are described as follows.

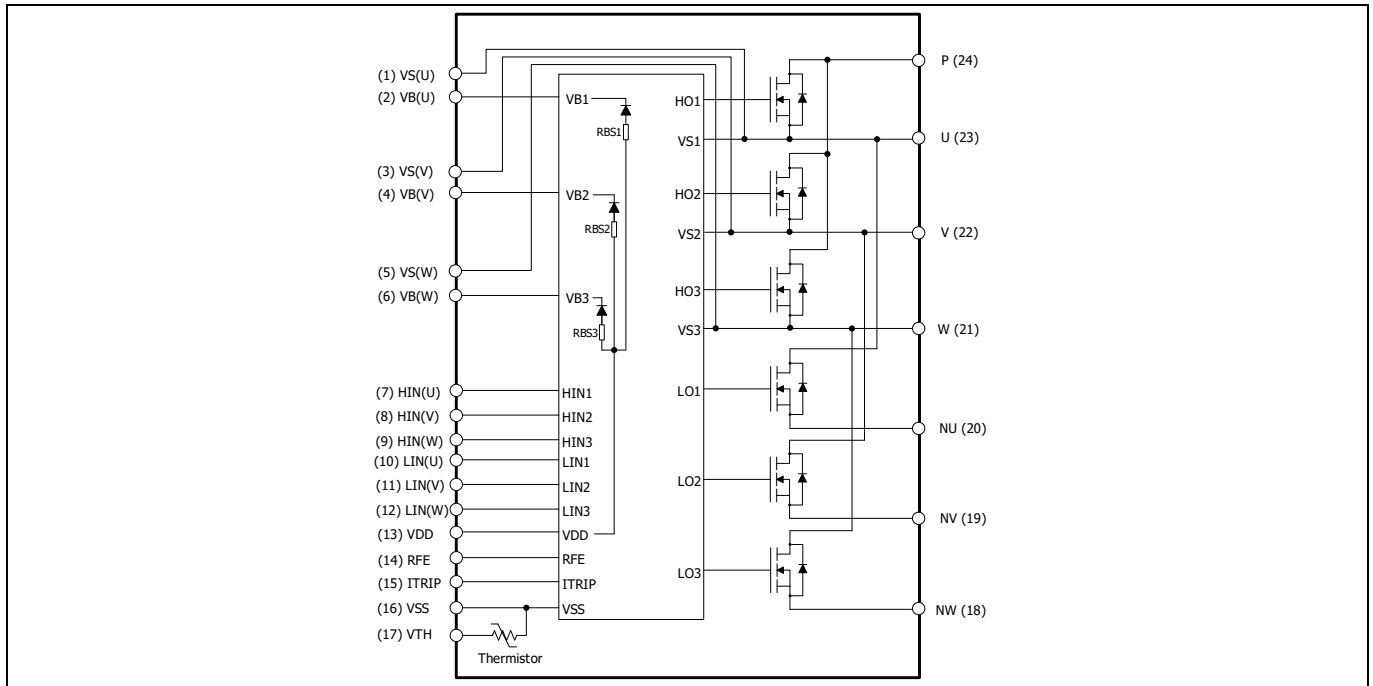


Figure 3 Internal circuit (3-phase inverter with open source)

Features

- 1200 V 20 A rating
- Fully isolated DIL molded module with DCB substrate
- CoolSiC™ 1200 V SiC MOSFETs
- Rugged 1200 V SOI gate driver technology with stability against transient and negative voltage
- Integrated bootstrap diode
- Matched delay times of all channels / built-in deadtime
- Lead-free terminal plating; RoHS compliant

Functions

- Overcurrent shutdown
- Built-in, UL-certified NTC thermistor for temperature monitoring
- Under-voltage lockout at all channels
- Low-side source pins accessible for current monitoring
- Anti cross-conduction function
- All six switches turn off during protection
- Programmable fault clear timing and enable input

3.2 Maximum electrical ratings

Table 2 Detailed description of absolute maximum ratings (IM828-XCC)

Item	Symbol	Rating	Description
Max. blocking voltage	V_{DSS}	1200 V	The sustained drain-source voltage of internal MOSFETs
*DC drain current	I_D	± 35 A	The allowable MOSFET DC drain current at $T_C = 25^\circ\text{C}$.
		± 20 A	The allowable MOSFET DC drain current at $T_C = 80^\circ\text{C}$.
Junction temperature	T_J	$-40 \sim 150^\circ\text{C}$	Considering temperature ripple on the power chips, the maximum junction temperature rating of the IPM is 150°C . (Maximum T_J of MOSFET itself can be 175°C , however IPM included not only MOSFET but also gate driver IC. Therefore, maximum T_J of IPM is just 150°C .)
Operating case temperature range	T_C	$-40 \sim 125^\circ\text{C}$	T_C (case temperature) is defined as the temperature of the package surface underneath the specified power chip. Please mount a temperature sensor on a heat sink surface at the defined position in Figure 4, so as to get accurate temperature information.

*Note: Pulse width and period are limited by junction temperature.

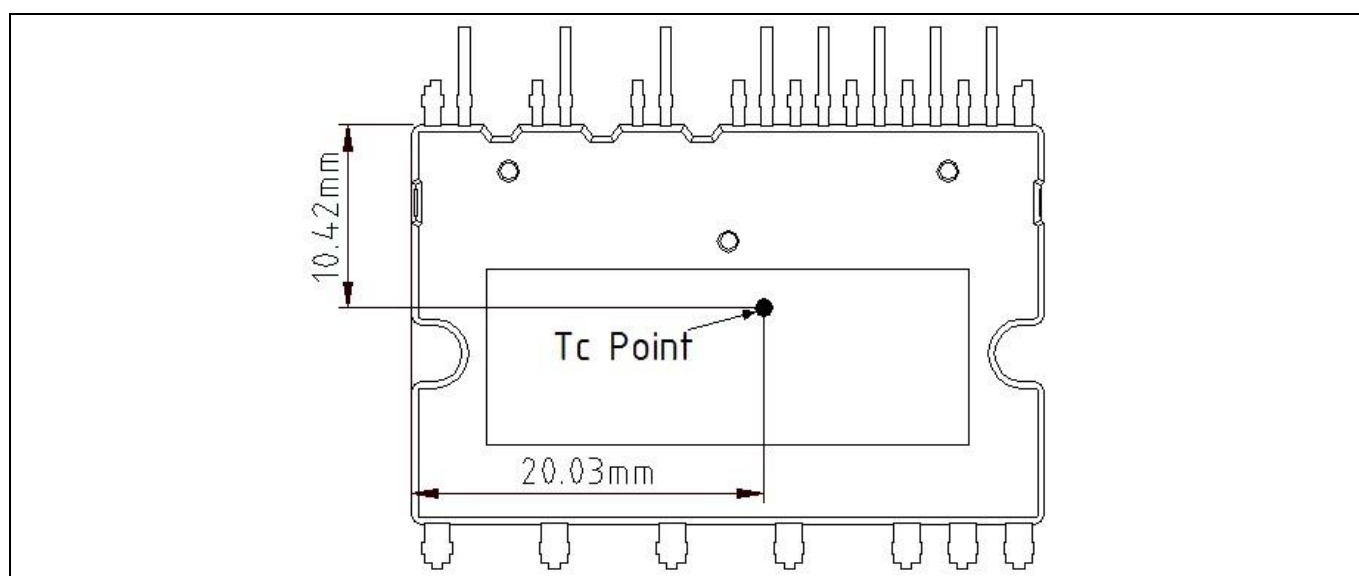


Figure 4 T_C measurement point (unit [mm])

3.3 Electrical characteristics

3.3.1 Statics characteristics

The static characterization includes blocking capability, output characteristics, $R_{DS(on)}$ vs. T_J , and body diode I-V characteristics.

3.3.1.1 Blocking capability

The leakage current I_{DSS} of IM828-XCC is measured with increasing temperature at a blocking voltage 1200 V. This was done by $V_{DD} = 0$ V, and thus the device is off. At a blocking voltage of 1200 V, each device's leakage current I_{DSS} is typically at 2 μ A at 25°C and 4 μ A at 150°C.

3.3.1.2 Output characteristics

The I-V curves, or output characteristics, of each MOSFET on IM828-XCC are measured in pulse mode for different junction temperatures of 25°C and 150°C, respectively. Figure 6 (left) shows the drain current as a function of drain source voltage V_{DS} with different V_{DD} . The solid curves are typical results at 25°C and the dashed curves are the ones at the maximum junction temperature of 150°C. The device is designed for an on-state gate voltage of +15 V, which is common for Si IGBT. The typical on-resistance of the device is determined at $V_{DD} = +15$ V and a rated current of $I_D = 20$ A. It amounts $R_{DS(on)} = 55$ m Ω at $T_J = 25^\circ\text{C}$. (The $R_{DS(on)}$ of IM828-XCC included not only SiC MOSFET $R_{DS(on)}$ (typ. 45 m Ω) but also package parasitic resistance (approximately 10 m Ω .) due to bonding wire and lead frame.)

As the SiC MOSFET is a voltage-controlled device, it turns on step by step with increasing gate source voltage V_{GS} . The higher gate source voltage is above threshold level, the higher drain current is at given drain voltage. The curves of Figure 6 are almost linear up to drain currents of about 30 A if the gate source voltage is above 13 V. For higher drain currents or lower gate source voltages, there is a significant curvature steadily lowering the current slope with increasing V_{DS} . This behavior is a consequence of the built-in JFET which is formed by the deep p+ wells (see Figure 5). As the p+ wells are linked to source, the junction channel of the JFET is controlled by drain-source voltage drop. Hence, the JFET channel is narrowed down with increasing V_{DS} . This feature improves the short-circuit ruggedness by limiting the saturation current for very high drain voltages V_{DS} .

The temperature behavior of the I-V characteristic depends also on temperature: above 13 V of control supply voltage V_{DD} , the drain current decreases with temperature. Below 13 V control supply voltage V_{DD} , the drain current increases with temperature, this is not recommended to have V_{DD} below +13 V for on-state. However, IM828-XCC have V_{DD} and V_{BS} undervoltage lock out UVLO functionality to prevent operation with low gate voltage. In general, the device could be driven with higher V_{DD} than 15 V, which further improves the on-state behavior. However, the lifetime of the gate oxide will be reduced since the gate oxide stress is higher thus accelerating the aging of the device. Consequently the failure rate can be increased by using a higher control supply voltage than 15 V. For on-state operating, Infineon recommends $V_{DD} = +15$ V of its IM828-XCC. The trade-off between long lifetime and low drain voltage V_{DS} is balanced in an optimum manner for this on-state operation voltage. For more information, refer to reference document.^[9]

Product overview

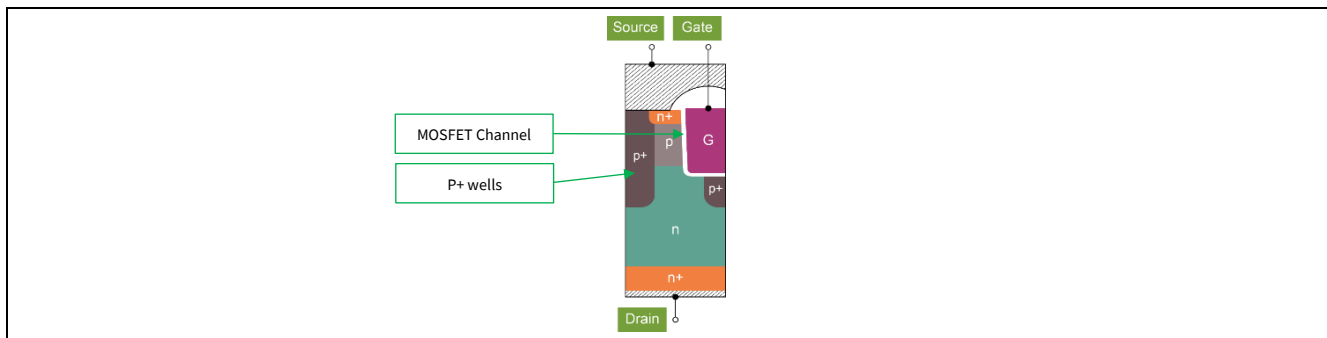


Figure 5 Sketch of the CoolSiC™ MOSFET cell

3.3.1.3 On-state resistance $R_{DS(on)}$ vs. junction temperature T_J

The on-state resistance $R_{DS(on)}$ is shown below in Figure 6 (right) as a function of junction temperature T_J with drain-to-source current I_D as a parameter. At 20 A and 25°C, the typical value of $R_{DS(on)}$ is 55 mΩ with $V_{DD} = +15$ V. The $R_{DS(on)}$ of CoolSiC™ MOSFET is mainly determined by three parts: MOSFET's channel, intrinsic JFET and drift region in the device, which are all temperature dependent. The MOSFET's channel has a negative temperature characteristics due to the behavior of the interface states, while drift region and intrinsic JFET have positive temperature characteristic. Because of the advantageous channel orientation along the preferred crystal plane with a low density of interface defects, the total $R_{DS(on)}$ of CoolSiC™ MOSFET is not dominated by the MOSFET's channel resistance, and it monotonously increases with temperature as the physics of MOSFETs with superior channel quality predict. This behavior is beneficial to balance the current distribution of parallel devices. Moreover, with high temperature, the $R_{DS(on)}$ is increased to limit the highest saturation current, and thus improve the short circuit ruggedness of the device as well.

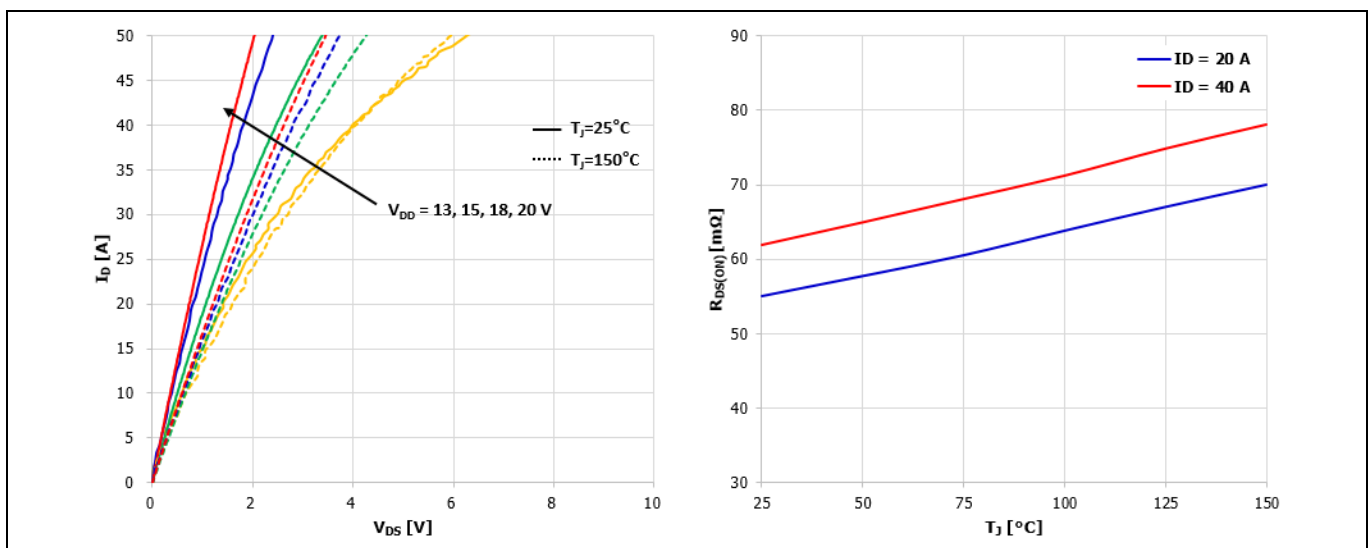


Figure 6 (Left) Typical output characteristic, V_{DD} as parameter, with $T_J = 25^\circ\text{C}$ and $T_J = 150^\circ\text{C}$; (Right) Typical on-resistance vs. junction temperature, I_D as parameter ($V_{DD} = 15$ V)

3.3.1.4 3rd quadrant operating mode

Like other MOSFETs, the CoolSiC™ MOSFET also integrates an intrinsic body diode with p-n junction behavior. As shown in Figure 7, the intrinsic bipolar body diode has high forward voltage V_{SD} (about 4.1 V at 20 A) if the control supply voltage is 0 V. This is due to the wide bandgap characteristics of the silicon carbide material. The forward voltage V_{SD} has a negative temperature coefficient as well as the standard Si p-n junction diode. So it is

Product overview

not useful using its body diode to conduct current for long cycle periods. However, the body diode has to operate during the deadtime when both high-side and low-side MOSFETs are turned off for bridge topology, and to reduce the on-state conduction losses due to the body diode, it is necessary to design the deadtime as short as possible. The value of deadtime depends on the topologies and design circuit, for example, hard-switching or soft-switching, PCB layout, gate drive IC selection, and etc. It can range from one hundred nanoseconds to several hundred nanoseconds.

Fortunately, unlike an IGBT, the SiC MOSFET can conduct reverse current from source to drain through the channel, if a positive bias is applied to the gate. This mode of operation is called synchronous rectification (or 3rd quadrant operation) and is achieved with a positive voltage of typically +15 V on the gate. As shown in the figure below, this synchronous rectification mode is highly recommended in order to limit the conduction loss. Also, with synchronous rectification mode, another benefit is to have a positive temperature coefficient with the ease of the devices' paralleling operation, which is the same as the 1st quadrant output I-V operation mentioned in Section 3.3.2.1. Table 3 shows the static characteristics of IM828-XCC.

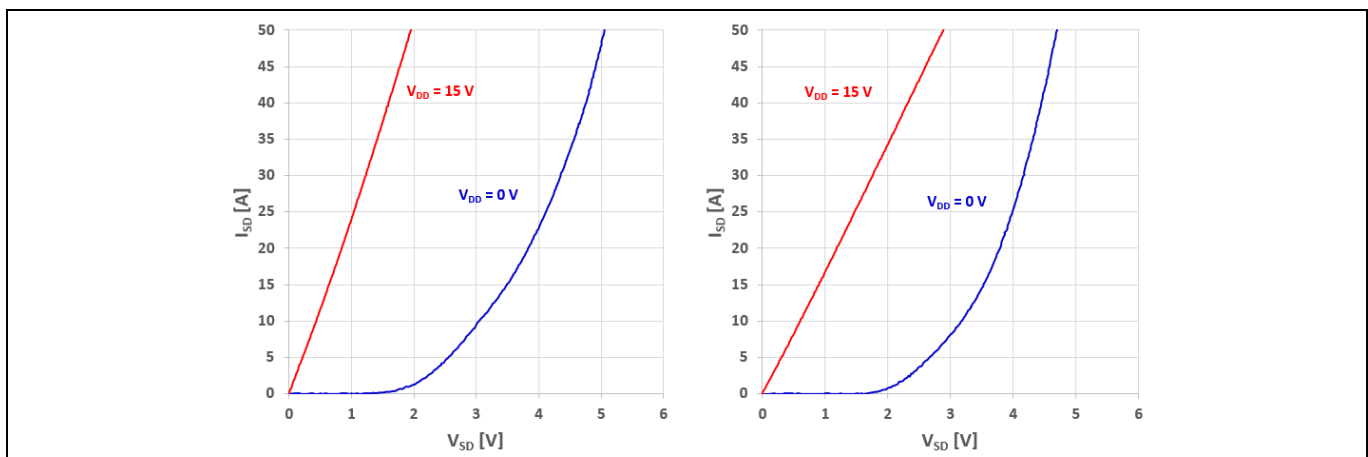


Figure 7 Reverse current I_{SD} as function of voltage at different V_{DD} and temperature: $T_J = 25^\circ\text{C}$ (left), $T_J = 150^\circ\text{C}$ (right)

Table 3 Static characteristics of IM828-XCC (at $V_{DD} = V_{BS} = 15\text{ V}$)

Description	Symbol	Condition		Value			Unit
				Min.	Typ.	Max.	
Drain-source on-state resistance	$R_{DS(on)}$	$V_{IN} = 5\text{ V}$ $I_D = 20\text{ A}$	$T_J = 25^\circ\text{C}$	-	55	87	$\text{m}\Omega$
			$T_J = 150^\circ\text{C}$	-	70	-	
Drain-source leakage current	I_{DSS}	$V_{DS} = 1200\text{ V}$		-	-	1	mA
Diode forward voltage	V_{SD}	$V_{IN} = 0\text{ V}$ $I_{SD} = 20\text{ A}$	$T_J = 25^\circ\text{C}$	-	3.9	5.8	V
			$T_J = 150^\circ\text{C}$	-	3.8	-	

3.3.2 Dynamic characteristics

The dynamic characterization includes the switching characteristics, body diode reverse recovery characteristics, and short circuit ruggedness.

3.3.2.1 Switching characteristics

The CoolSiC™ MOSFET on IM828-XCC is needed to consider the on-state and off-state control supply voltage V_{DD} voltage at first. For the turn-on V_{DD} voltage of on-state operating, as mentioned in the previous section, +15 V is recommended to trade-off between long lifetime and low forward voltage, which is also a common turn-on voltage in common Si IGBTs. In order to ensure low conduction loss, the supply of the gate driver should be stabilized for maintaining the on-state V_{DD} at 15 V ideally. For the turn-off V_{DD} voltage of off-state operating, the SiC MOSFET itself is capable of switching at a very high speed and the voltage slew rate can range from tens to a hundred of volts per nanosecond. In order to improve the noise interference immunity, a negative gate-to-source turn-off voltage is normally recommended. However, the slew rate of IM828-XCC is designed to a few volts per nanosecond for three-phase inverter applications by the internal SOI gate driver IC. Therefore, IM828-XCC is allowed off-state operating with $V_{GS} = 0$ V because of the high robustness threshold voltage $V_{GS(th)}$ of the CoolSiC MOSFET.

The switching time definition and evaluation method are shown in Figure 8(a) and (b). The inductive load switching test circuit is used to measure the switching losses for $V_{DD} = 15$ V at 150°C as shown in Figure 9(left). The recommended control supply voltage V_{DD} (gate source voltage V_{GS}) of IM828-XCC is 15 V.

Under the same operating conditions, IM828-XCC shows much less switching losses compared to its conventional Si IGBT IPM as Figure 9 (right). In addition, IM828-XCC can achieve better switching performance (E_{on} by 18% and E_{off} by around 2% at drain current to 40 A) with higher control supply voltage V_{DD} (18V) without the SiC MOSFET degradation impact^[9] as shown in Figure 9(left and center). Figure 10 shows a typical switching waveform of IM828-XCC at inductive load-switching test conditions as in Figure 8(b). However, it should also be considered that the short-circuit peak current is much higher compared to the 15 V turn-on voltage as shown in Figure 13. Therefore, the short-circuit capability of the IM828-XCC at 18 V turn-on voltage will be worse than at 15 V turn-on voltage.

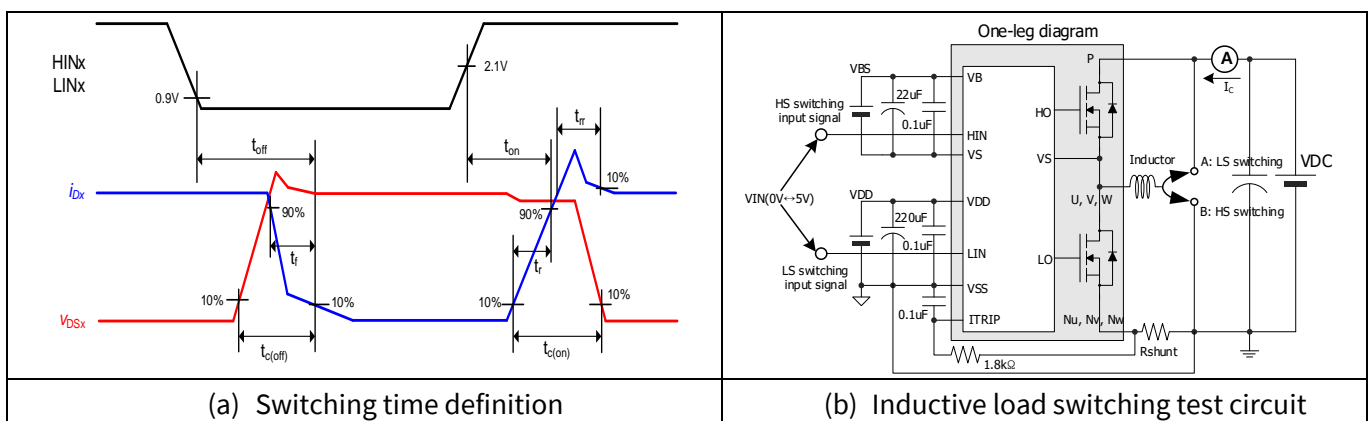


Figure 8 Switching time definition and evaluation circuit for switching test

Product overview

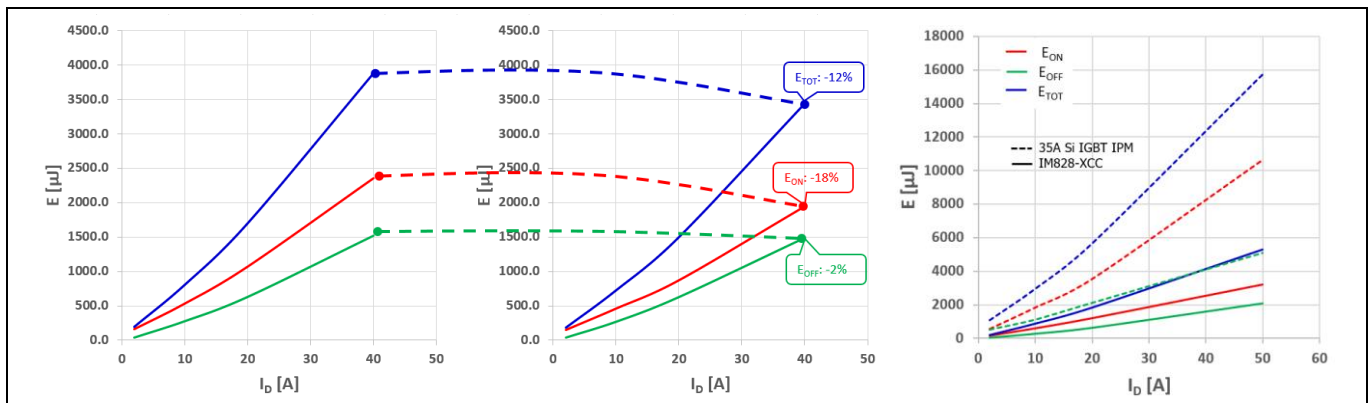


Figure 9 Typical switching energy losses at $T_J = 150^\circ\text{C}$; $V_{DD} = 15\text{ V}$ (left) and $V_{DD} = 18\text{ V}$ (center), and typical switching energy losses comparison between IM828-XCC and 35A Si IGBT IPM (right)

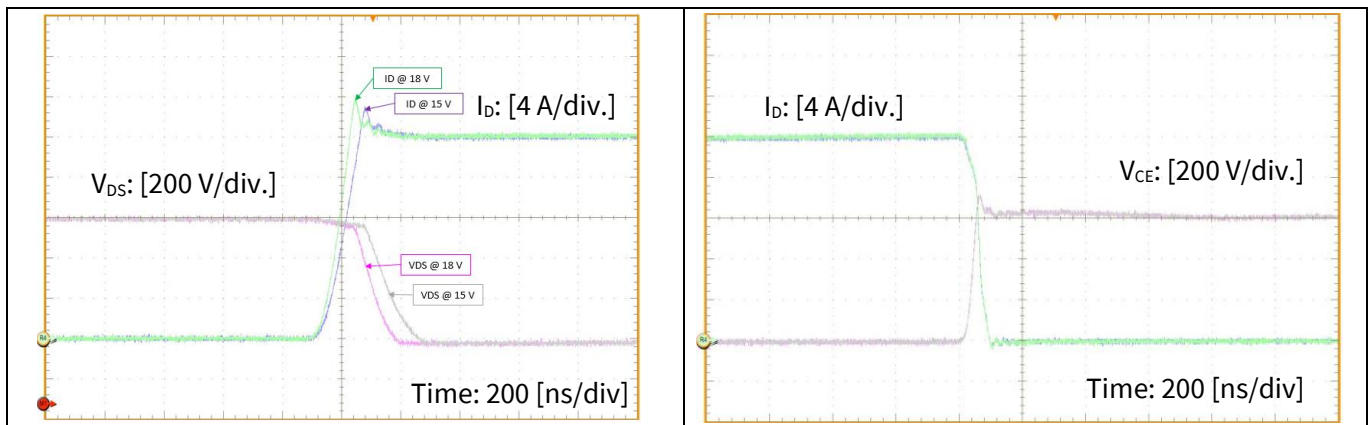


Figure 10 IM828-XCC typical switching waveform; turn-on(left) and turn-off(right) ($V_{DC} = 600\text{ V}$, $V_{DD} = 15 / 18\text{ V}$, $I_D = 20\text{ A}$, $T_J = 150^\circ\text{C}$, inductive load = 3 mH)

Product overview

Table 4 and Table 5 shows dynamic characteristics and switching losses of IM828-XCC.

Table 4 Dynamic characteristics of IM828-CC (at $V_{DD} = 15\text{ V}$, $T_J = 25^\circ\text{C}$)

Description		Symbol	Condition	Value			Unit
				Min.	Typ.	Max.	
High side	Turn-on propagation delay time	t_{on}	$V_{LIN, HIN} = 0\text{ V} \rightarrow 5\text{ V}$, $I_D = 20\text{ A}$, $V_{DC} = 600\text{ V}$	-	870	-	ns
	Turn-on rise time	t_r		-	45	-	ns
	Turn-on switching time	$t_{c(on)}$		-	140	-	ns
	Reverse recovery time	t_{rr}		-	60	-	ns
	Turn-off propagation delay time	t_{off}	$V_{LIN, HIN} = 5\text{ V} \rightarrow 0\text{ V}$, $I_D = 20\text{ A}$, $V_{DC} = 600\text{ V}$	-	960	-	ns
	Turn-off fall time	t_f		-	70	-	ns
	Turn-off switching time	$t_{c(off)}$		-	100	-	ns
Low side	Turn-on propagation delay time	t_{on}	$V_{LIN, HIN} = 0\text{ V} \rightarrow 5\text{ V}$, $I_D = 20\text{ A}$, $V_{DC} = 600\text{ V}$	-	960	-	ns
	Turn-on rise time	t_r		-	85	-	ns
	Turn-on switching time	$t_{c(on)}$		-	230	-	ns
	Reverse recovery time	t_{rr}		-	90	-	ns
	Turn-off propagation delay time	t_{off}	$V_{LIN, HIN} = 5\text{ V} \rightarrow 0\text{ V}$, $I_D = 20\text{ A}$, $V_{DC} = 600\text{ V}$	-	880	-	ns
	Turn-off fall time	t_f		-	50	-	ns
	Turn-off switching time	$t_{c(off)}$		-	60	-	ns

Table 5 Switching loss of IM828-XCC (at $V_{DC} = 600\text{ V}$, $V_{DD} = 15\text{ V}$, $I_D = 20\text{ A}$)

Description		Symbol	Condition	Value			Unit
				Min.	Typ.	Max.	
High side	MOSFET turn-on energy (includes reverse recovery of diode)	E_{on}	$T_J = 25^\circ\text{C}$	-	0.90	-	mJ
			$T_J = 150^\circ\text{C}$		1.04		mJ
	MOSFET turn-off energy	E_{off}	$T_J = 25^\circ\text{C}$	-	0.48	-	mJ
			$T_J = 150^\circ\text{C}$	-	0.66	-	mJ
	Body diode recovery energy	E_{rec}	$T_J = 25^\circ\text{C}$	-	0.08	-	mJ
			$T_J = 150^\circ\text{C}$		0.10		mJ
Low side	MOSFET turn-on energy (includes reverse recovery of diode)	E_{on}	$T_J = 25^\circ\text{C}$	-	1.51	-	mJ
			$T_J = 150^\circ\text{C}$		1.62		mJ
	MOSFET turn-off energy	E_{off}	$T_J = 25^\circ\text{C}$	-	0.25	-	mJ
			$T_J = 150^\circ\text{C}$	-	0.34	-	mJ
	Body diode recovery energy	E_{rec}	$T_J = 25^\circ\text{C}$	-	0.07	-	mJ
			$T_J = 150^\circ\text{C}$		0.07		mJ

3.3.2.2 Body diode reverse recovery characteristics

The intrinsic body diode switching performance of SiC MOSFET is measured with $V_{DS}=600\text{ V}$, $V_{DD}=15\text{ V}$ and $I_D = 20\text{ A}$. Figure 11 is reverse recovery losses E_{rr} and reverse recovery current I_{rr} as a function of diode current slope for IM828-XCC based on CoolSiC™ SiC MOSFET body diode dynamic characteristics.

From Figure 11, unlike the SiC Schottky diode, the reverse recovery losses (E_{rr}) is temperature dependent; the higher the temperature, the higher the reverse recovery losses. Obviously, this is an effect due to minority carriers injected by the forward biased intrinsic pn-junction, which generates a reverse recovery charge. Fortunately, the absolute values at the rated current are still fairly low, meaning the CoolSiC™ MOSFET has negligible reverse recovery losses.

The body diode E_{rr} is an important parameter for bridge topology with hard switching. During the deadtime period of bridge topology, the body diode is freewheeling current before the corresponding switch is turned on, and when this corresponding switch is turned on, the body diode reverse recovery current will go through the corresponding switch in a short period. With the low E_{rr} of CoolSiC™ SiC MOSFET, it can minimize the switching loss and increase the switching frequency.

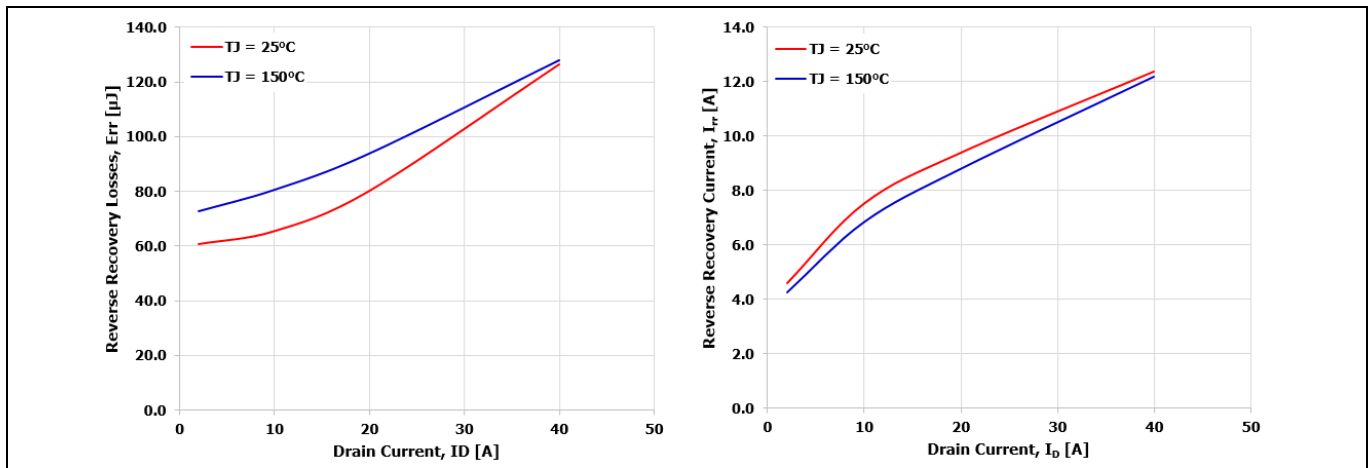


Figure 11 Typical reverse recovery losses (left) and reverse recovery current (right) as a function of diode current slope for IM828-XCC

3.3.2.3 SCSOA(short-circuit safe operation area) characteristics

Figure 12 shows the typical (not guaranteed) SCSOA performance graph of IM828 products under the short circuit status with the following conditions. In the case of IM828-XCC, the graph illustrates that if the short circuit time is less than 3.8 μs , the SiC MOSFET has the ability to turn off safely. In this case, the SiC MOSFET can shut down an SC current (non-repetitive) about 346 A_{peak} under a control supply voltage of 18.0 V. Figure 13 shows typical SC (short circuit) waveform at DC link voltage $V_{\text{DC}} = 800 \text{ V}$, control power supply voltage $V_{\text{DD}} = 15 \text{ V}$ / 18 V, and $T_J = 150^\circ\text{C}$.

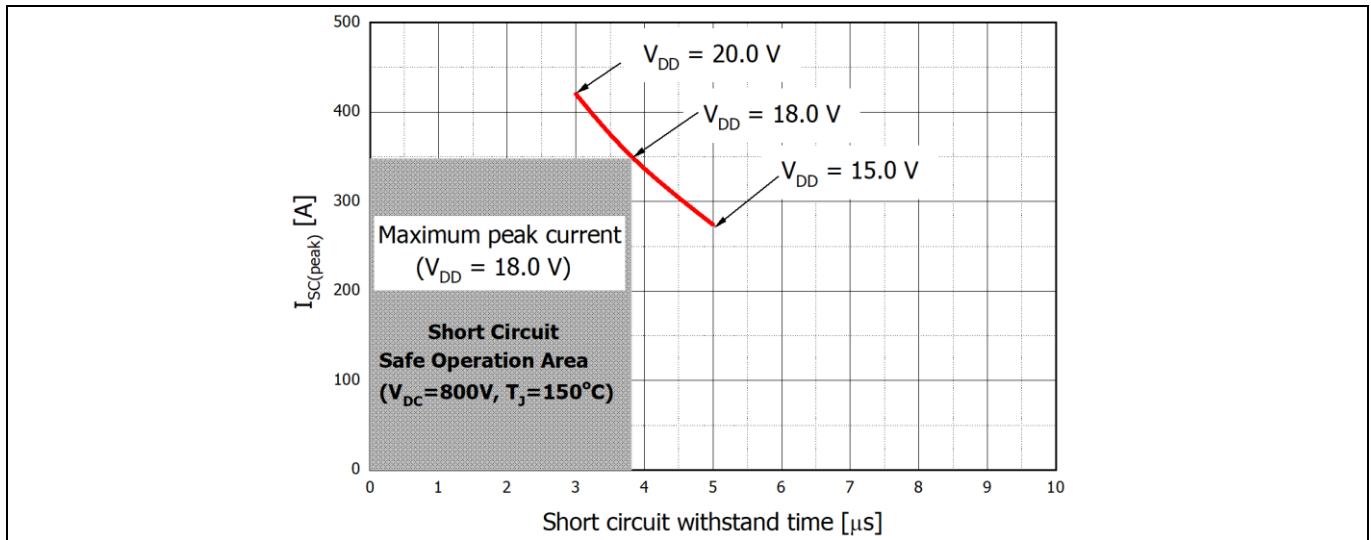


Figure 12 Typical SCSOA graph of IM828-XCC (at $V_{\text{DC}} = 800 \text{ V}$, $V_{\text{PN(surge)}} < 1200 \text{ V}$, $T_J = 150^\circ\text{C}$)

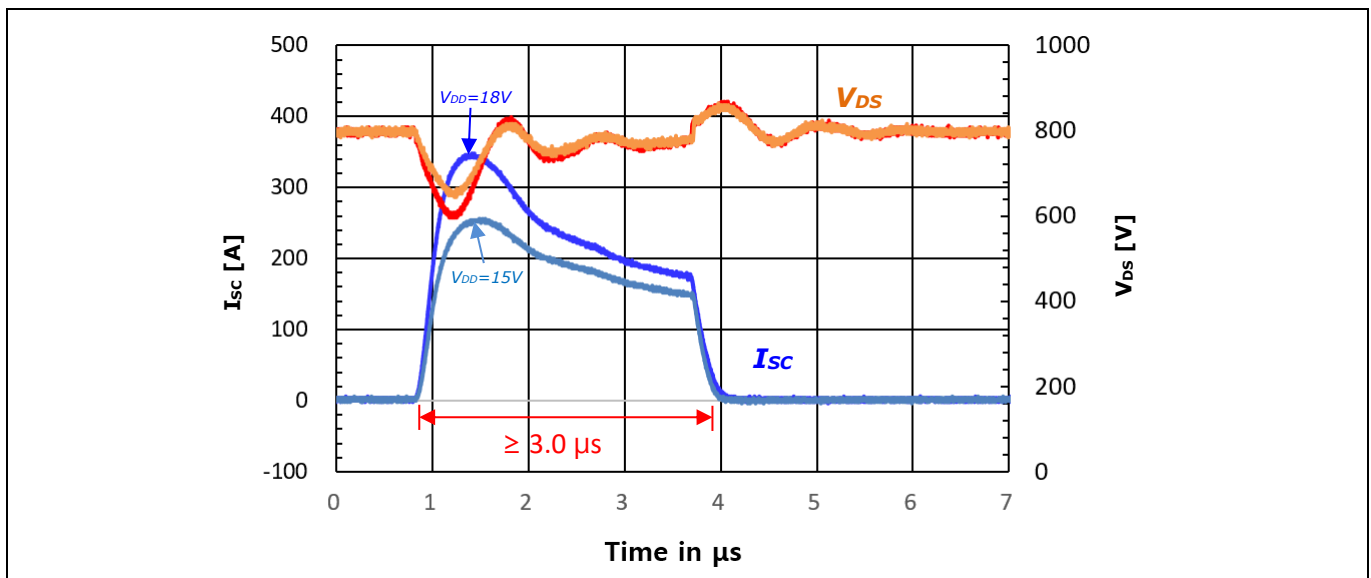


Figure 13 Typical short circuit (SC) waveform of IM828-XCC ($V_{\text{DC}} = 800 \text{ V}$, $V_{\text{DD}} = 15 \text{ V} / 18 \text{ V}$, $T_J = 150^\circ\text{C}$)

3.4 Description of the input and output pins

Table 6 defines the IM828 input and output pins. The detailed functional descriptions are as follows:

Table 6 Pin descriptions of IM828

Pin Number	Pin Name	Pin Description
1	VS(U)	U-phase high side floating IC supply offset voltage
2	VB(U)	U-phase high side floating IC supply voltage
3	VS(V)	V-phase high side floating IC supply offset voltage
4	VB(V)	V-phase high side floating IC supply voltage
5	VS(W)	W-phase high side floating IC supply offset voltage
6	VB(W)	W-phase high side floating IC supply voltage
7	HIN(U)	U-phase high side gate driver input
8	HIN(V)	V-phase high side gate driver input
9	HIN(W)	W-phase high side gate driver input
10	LIN(U)	U-phase low side gate driver input
11	LIN(V)	V-phase low side gate driver input
12	LIN(W)	W-phase low side gate driver input
13	VDD	Low side control supply
14	RFE	Programmable fault clear time, fault output, enable input
15	ITRIP	Overcurrent shutdown input
16	VSS	Low side control negative supply
17	VTH	NTC thermistor terminal
18	NW	W-phase low side source
19	NV	V-phase low side source
20	NU	U-phase low side source
21	W	Motor W-phase output
22	V	Motor V-phase output
23	U	Motor U-phase output
24	P	Positive bus input voltage

High-side bias voltage pins for driving the MOSFET

Pins: VB (U, V, W) – VS (U, V, W)

- These pins provide the gate-drive power to the high-side MOSFETs.
- The ability to utilize a bootstrap circuit scheme for the high-side MOSFETs eliminates the need for external power supplies.
- Each bootstrap capacitor is charged from the VDD supply during the ON-state of the corresponding low-side MOSFET or the freewheeling state of the low-side body diode.
- In order to prevent malfunctions caused by noise and ripple in the supply voltage, a good-quality (low ESR, low ESL) filter capacitor should be mounted very close to these pins.

Product overview

Low side-bias voltage pin

Pin: VDD

- This is the control supply pin for the internal IC.
- In order to prevent malfunctions caused by noise and ripples in the supply voltage, a good-quality (low ESR, low ESL) filter capacitor should be mounted very close to this pin.

Low-side, common-supply ground pin

Pin: VSS

- This pin connects the control ground for the internal IC.

Signal input pins

Pins: HIN (U, V, W), LIN (U, V, W)

- These are pins used to control the operation of the internal MOSFETs.
- They are activated by voltage input signals. The terminals are internally connected to a Schmitt trigger circuit composed of 3.3 V/5 V-class CMOS.
- The signal logic of these pins is active-high. The MOSFET associated with each of these pins will be turned "ON" when a sufficient logic voltage is applied to these pins.
- The wiring of each input should be as short as possible to protect the IM828 against noise influences.
- To prevent signal oscillations, an RC coupling is recommended as illustrated in Figure 15.

Overcurrent detection pin

Pin: ITRIP

- The current sensing shunt resistor should be connected between the N pin (source of low-side MOSFET) and the power ground to detect short-circuit current (refer to Figure 20). An RC filter should be connected between the shunt resistor and the ITRIP pin to eliminate noise.
- The integrated comparator is triggered if the voltage V_{ITRIP} is higher than 0.5 V. The shunt resistor should be selected to meet this level for the specific application. In case of a trigger event, the voltage at the RFE pin is pulled down to LOW.
- The connection length between the shunt resistor and ITRIP pin should be minimized.

Fault output, fault-clear time, and enable pin

Pin: RFE

- The fault-out indicates a module failure in case of undervoltage at pin VDD or in case of triggered overcurrent detection at ITRIP. The alarm conditions are overcurrent detection and low-side bias UV (undervoltage) operation.
- The programmable fault-clear time can be adjusted by the RC network, which is an external pull-up resistor and capacitor. For example, the typical value is about 1 ms at 1 M Ω and 2 nF.
- The microcontroller can pull this pin low to disable the IPM functionality. This is the enable function.

Product overview

NTC thermistor terminal pin

Pin: VTH

- This is the NTC thermistor terminal pin
- This pin provides direct access to the NTC thermistor, which is referenced to VSS. An external pull-up resistor connected to +5 V ensures that the resulting voltage can be directly connected to the microcontroller.

Positive DC-link pin

Pin: P

- This is the DC-link positive-power supply pin.
- It is internally connected to the collectors of the high-side MOSFETs.
- In order to suppress the surge voltage caused by the DC-link wiring or PCB pattern inductance, connect a smoothing filter capacitor close to this pin. (Typically metal film capacitors are used.)

Negative DC-link pins

Pins: NU, NV, NW

- These are the DC-link negative-power supply pins (power ground) of the inverter.
- These pins are connected to the low-side MOSFETs sources of the each phase.

Inverter power output pins

Pins: U, V, W

- Inverter output pins for connecting to the inverter load (e. g. motor).

3.5 Outline drawing

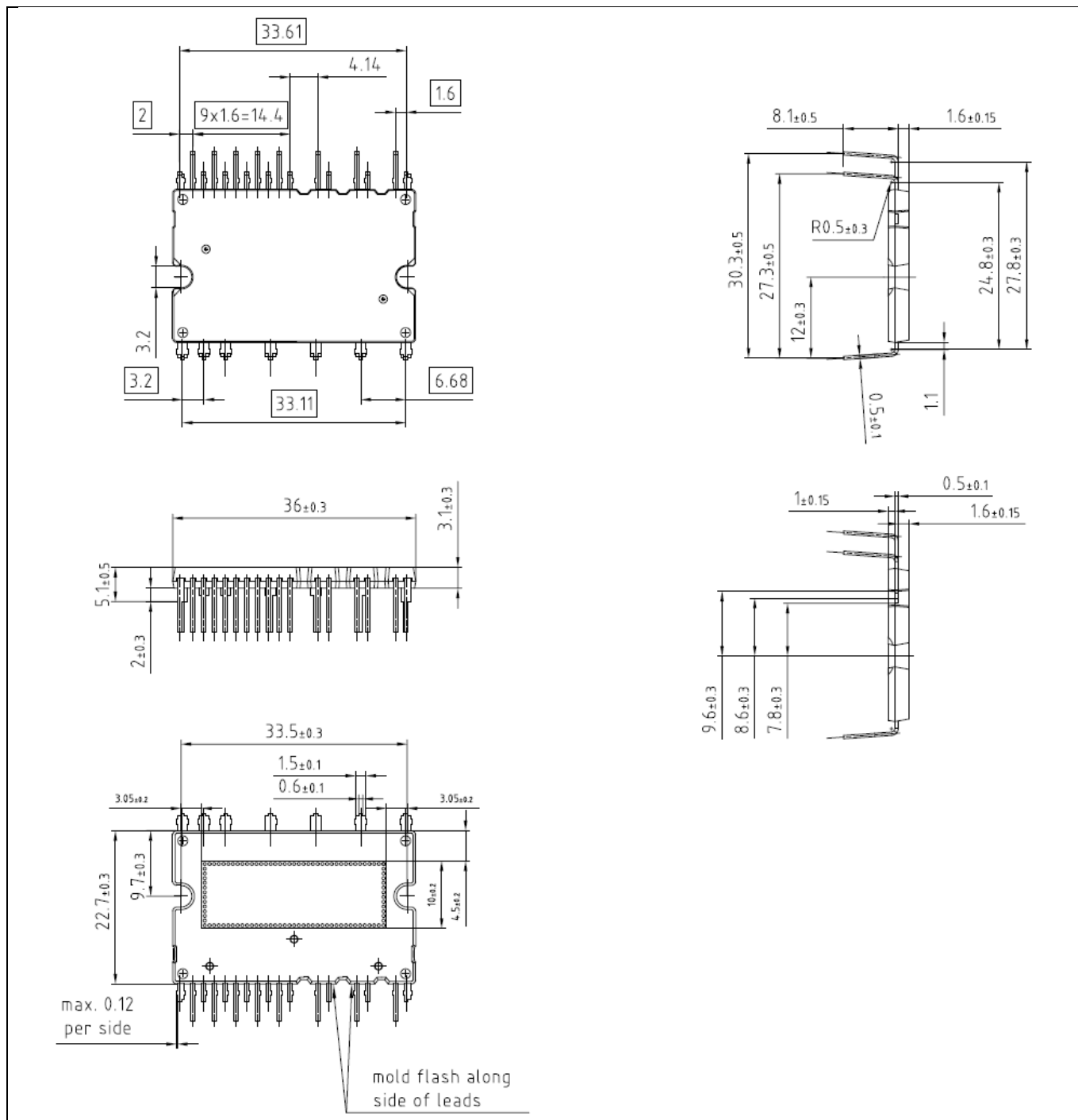


Figure 14 Package outline dimensions (Unit: [mm])

4 Interface circuit and layout guide

4.1 Input signal connection

Figure 15 shows the I/O interface circuit between micro-controller and IPM. The IPM input logic is active-high with internal pull-down resistors. External pull-down resistors are not needed.

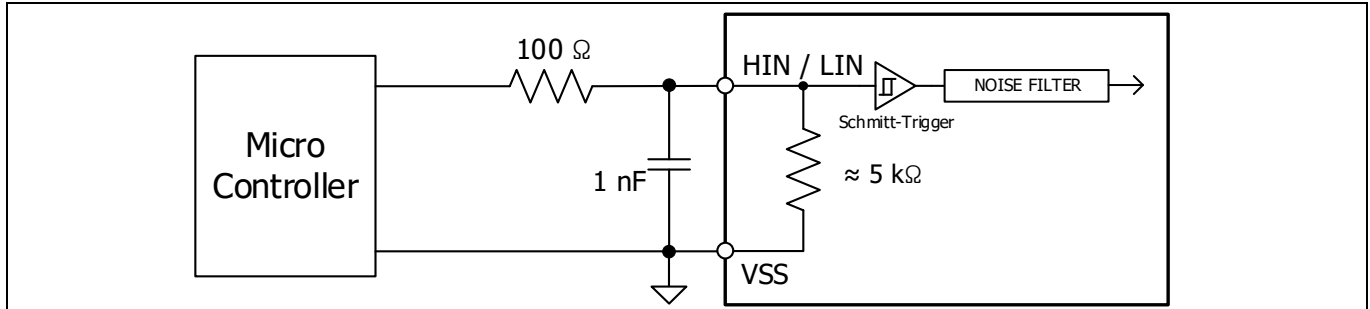


Figure 15 Recommended micro-controller I/O interface circuit

Table 7 Maximum ratings of inputs

Item	Symbol	Condition	Value	Unit
Module supply voltage	V_{DD}	Applied between $V_{DD} - V_{SS}$	-1 ~ 20	V
High- side floating supply voltage	V_{BS}	Applied between $V_B (U,V,W) - V_S (U,V,W)$	-1 ~ 20	V
Input voltage	V_{IN}	Applied between $HIN (U,V,W) - V_{SS}$, $LIN (U,V,W) - V_{SS}$	-1 ~ $V_{DD}+0.3$	V

The input maximum rating voltages are listed in Table 7. Since the input voltage rating is $V_{DD}+0.3$ V, a 15 V supply interface is possible. However, it is recommended that the input signal be configured with the 5 V or 3.3 V logic supply for direct connect with the micro-controller. It is recommended to place bypass capacitors as close as possible to the signal lines from the micro-controller as well as the IPM.

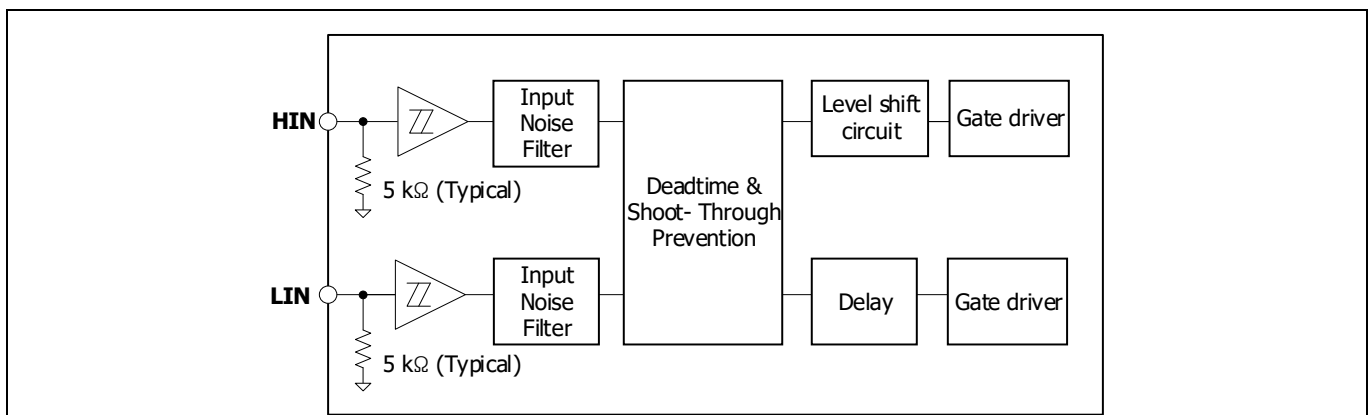


Figure 16 Simplified block diagram of IM828 gate driver IC

Because IM828 products employ active-high input logic, the power sequence restriction between the control supply and the input signal during start-up or shut-down operation does not exist. Therefore, it makes the system fail-safe. In addition, pull-down resistors are built into each input circuit. Thus, external pull-down resistors are not needed. This reduces the required external component count. Input Schmitt-trigger, noise

filter, deadtime and shoot-through prevention functions provide beneficial noise rejection to short input pulses. Furthermore, the inputs of IM828 are compatible with standard CMOS and TTL outputs. The gate driver IC of IM828 has been designed to be compatible with 3.3 V and 5 V logic-level signals. Therefore, by lowering the turn-on and turn-off threshold voltage of the input signal as shown in Table 8, a direct connection to 3.3 V / 5 V-class micro-controller or DSP is possible.

Table 8 Input threshold voltage (at VDD = 15 V, T_J = 25 °C)

Item	Symbol	Condition	Min.	Typ.	Max.	Unit
Logic "1" input voltage (LIN, HIN)	V _{IH}	HIN – VSS	-	1.9	2.3	V
Logic "0" input voltage (LIN, HIN)	V _{IL}	LIN – VSS	0.7	0.9	-	V

As shown in Figure 16, the IM828 input signal section integrates a 5 kΩ (typical) pull-down resistor. Therefore, when using an external filtering resistor between micro-controller output and IPM input, pay attention to the signal voltage drop at the IPM input terminals. It should fulfill the logic "1" input voltage requirement. For instance, R = 100 Ω and C = 1 nF for the parts shown in Figure 15.

4.2 Internal deadtime

The gate driver IC of IM828 features integrated deadtime protection circuitry. The deadtime for gate driver IC is fixed. The deadtime feature inserts a time period (a minimum deadtime) in which both the high- and low-side power switches are held off; this is done to ensure that the power switch being turned off has fully turned off before the second power switch is turned on.

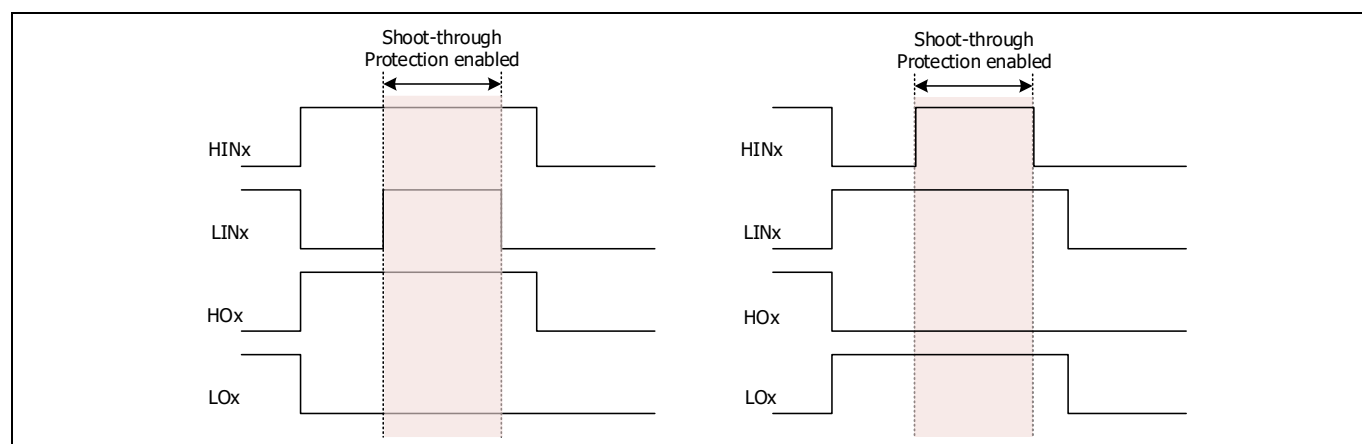
This minimum deadtime is automatically inserted whenever the external deadtime is shorter than DT_{IC}; external deadtimes larger than DT_{IC} are not modified by the gate driver IC.

Table 9 Internal deadtime (at VDD = 15 V, T_J = 25 °C)

Item	Symbol	Condition	Min.	Typ.	Max.	Unit
Internal deadtime	DT _{IC}	V _{IN} = 0 or V _{IN} = 5 V	300	-	-	ns

4.3 Cross-conduction prevention circuitry

The gate driver IC of IM828 is equipped with shoot-through protection circuitry (also known as cross-conduction prevention circuitry or interlock circuitry). Figure 17 shows how this protection circuitry prevents both the high- and low-side switches from conducting at the same time.


Figure 17 Illustration of shoot-through protection circuitry

4.4 Advanced input filter

The advanced input filter allows an improvement in the input/output pulse symmetry of the gate driver IC and helps to reject noise spikes and short pulses. This input filter has been applied to the HIN and LIN inputs. The working principle of the new filter is shown in Figure 18 (a), (b).

Figure 18 (a) shows a typical input filter and the asymmetry of the input and output. The upper pair of waveforms (Example 1) show an input signal width with a duration much longer then $t_{FIL,IN}$; the resulting output is approximately the difference between the input signal and $t_{FIL,IN}$. The lower pair of waveforms (Example 2) show an input signal with a duration slightly longer then $t_{FIL,IN}$; the resulting output is approximately the difference between the input signal and $t_{FIL,IN}$.

Figure 18 (b) shows the advanced input filter of IM828 and the symmetry between the input and output. The upper pair of waveforms (Example 1) show an input signal with a duration much longer then $t_{FIL,IN}$; the resulting output is approximately the same duration as the input signal. The lower pair of waveforms (Example 2) show an input signal with a duration slightly longer then $t_{FIL,IN}$; the resulting output is approximately the same duration as the input signal.

Table 10 Input filter time (at VDD = 15 V, T_J = 25 °C)

Item	Symbol	Condition	Min.	Typ.	Max.	Unit
Input filter time at LIN, HIN for turn-on and off	$t_{FIL,IN}$	$V_{LIN, HIN} = 0\text{ V or }5\text{ V}$	-	350	-	ns

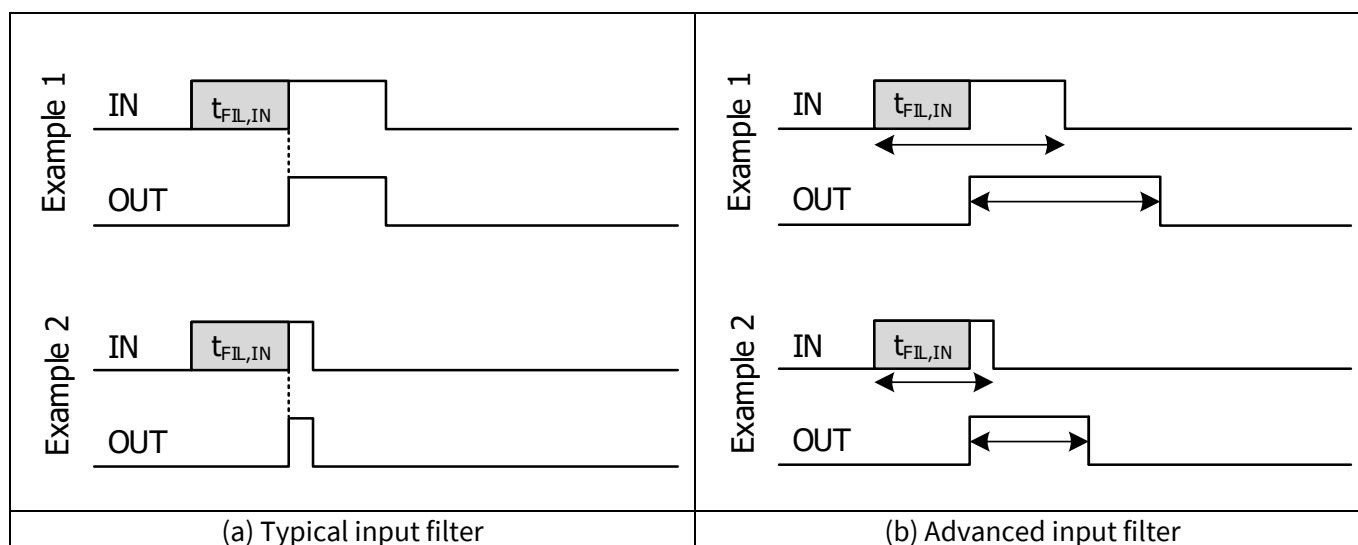


Figure 18 Internal Input filter characteristics

4.5 Matched propagation delay

The gate driver IC of IM828 is designed with propagation-delay matching circuitry. With this feature the internal gate driver IC's response at the output to a signal at the input requires approximately the same time duration (i.e., t_{ON} , t_{OFF}) for both the low-side channels and the high-side channels; the maximum difference is specified by the delay-matching parameter (M_T). The propagation turn-on delay (t_{ON}) of the IM828 is matched to the propagation turn-off delay (t_{OFF}). In other words, delay-matching turn-on/off between high-side and low-side means there is the time difference between the LO and HO outputs, when each output has reached 10% of its maximum (during turn-on), or when each output has decreased to 90% of its maximum (during turn-off), assuming that HINx and LINx are simultaneously applied. The shorter the delay-matching time, the better the circuit performance.

Table 11 Matching propagation delay time (at $V_{DD} = 15\text{ V}$, $T_J = 25^\circ\text{C}$)

Item	Symbol	Condition	Min.	Typ.	Max.	Unit
Matching propagation delay time (On & Off) all channels	M_T	External deadtime > 500 ns	-	-	130	ns

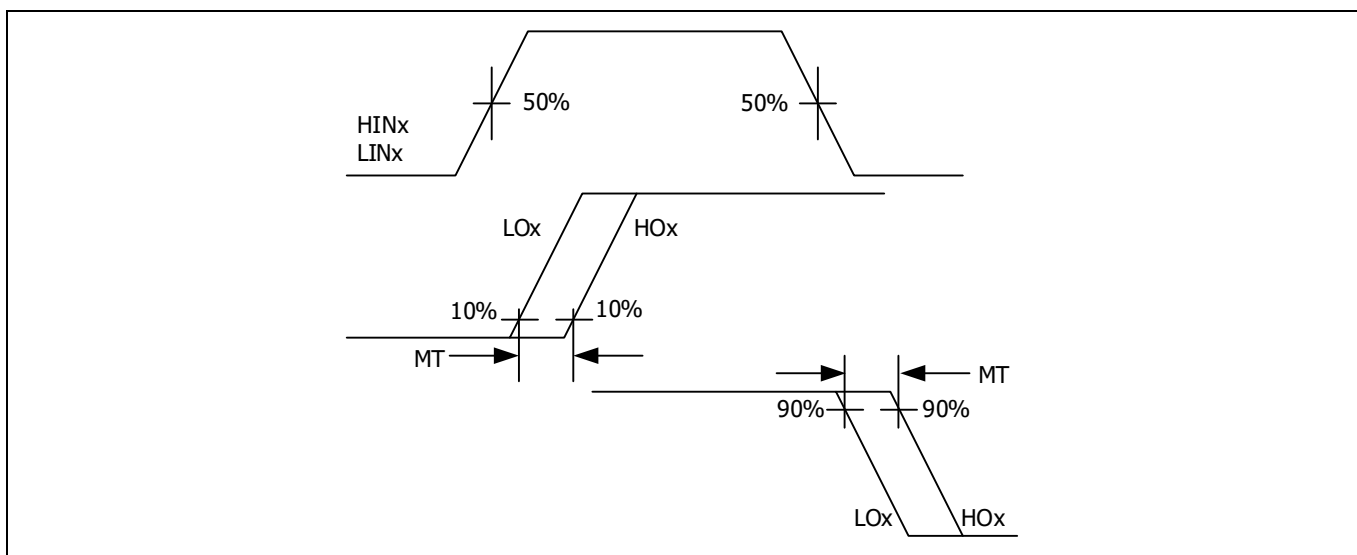


Figure 19 Delay-matching waveform definition

4.6 General interface circuit example

Figure 20 shows a typical application circuit of IM828 for interface schematic with control signals connected directly to a micro-controller.

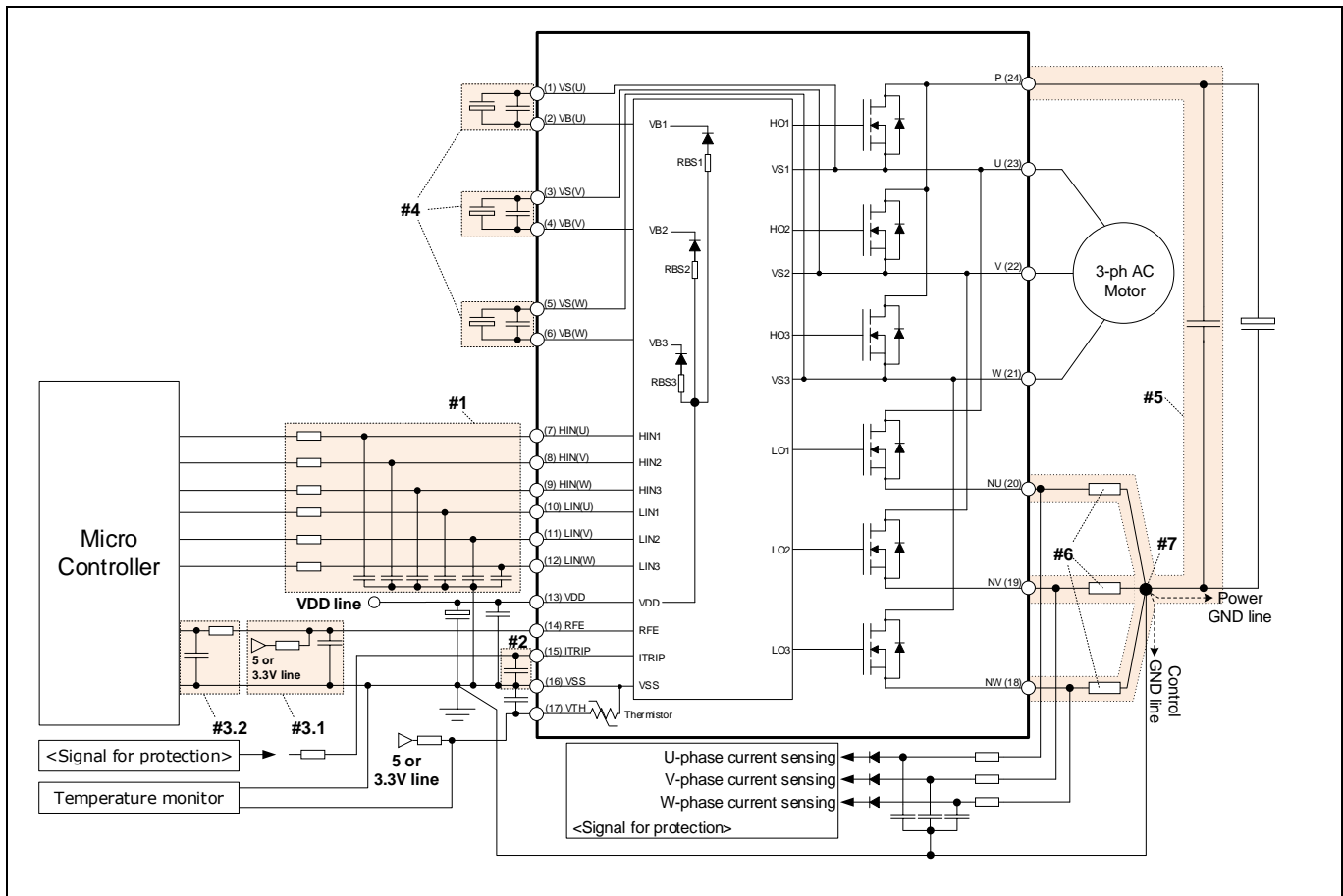


Figure 20 Application circuit example

Note:

1. Input circuit
 - To reduce input signal noise by high-speed switching, the R_{IN} and C_{IN} filter circuit should be mounted. (100 Ω , 1 nF)
 - C_{IN} should be placed as close to VSS pin as possible.
2. Itrip circuit
 - To prevent protection function errors, C_{ITRIP} should be placed as close to ITRIP and VSS pins as possible.
3. RFE circuit
 - 3.1 Pull-up resistor and pull-down capacitor
 - RFE output is an open-drain output. This signal line should be pulled up to the positive side of the 5 V / 3.3 V logic power supply with a proper resistor R_{PU} .
 - The fault-clear time is adjusted by RC network of a pull-up resistor, a pull-down capacitor and pull-up voltage.
 - $t_{FLTCLR} = -R_{pull-up} \cdot C_{pull-down} \cdot \ln(1 - V_{RFE,TH+} / V_{pull-up}) + \text{internal fault-clear time } 160 \mu s$
 - $t_{FLTCLR} = -1 M\Omega \times 2 nF \times \ln(1 - 1.9 / 5 V) + 160 \mu s \approx 1.1 ms$ at $R = 1 M\Omega$, $C = 2 nF$ and $V_{pull-up} = 5 V$
 - A pull-up resistor is limited to max. 2 M Ω
 - 3.2 RC filter
 - It is recommended that the RC filter be placed as close to the controller as possible.

4. VB-VS circuit
 - Capacitor for high-side floating supply voltage should be placed as close to VB and VS pins as possible.
5. Snubber capacitor
 - The wiring between IM828 and snubber capacitor including shunt resistor should be as short as possible.
6. Shunt resistor
 - The shunt resistor of SMD type should be used for reducing its stray inductance.
7. Ground pattern
 - Ground pattern should be separated at only one point of shunt resistor as short as possible.

4.7 Recommended rated output current of power supply

Control and gate drive power for the IM828 is normally provided by a single 15 V supply that is connected to the module VDD and VSS terminal. The circuit current of VDD control supply of IM828-XCC is shown in below Table 12.

Table 12 The circuit current of control power supply of IM828-XCC (Unit: [mA])

Item		Static (typ.)	Dynamic (typ.)	Total (typ.)
VDD = 15 V	FSW = 5 kHz	1.45	3.08	4.53
	FSW = 10 kHz	1.45	3.81	5.26
	FSW = 20 kHz	1.45	5.28	6.73
	FSW = 40 kHz	1.45	8.20	9.65
VDD = 20 V	FSW = 60 kHz	2.53	15.77	18.30

And, the circuit current of the 5 V logic power supply (RFE & input terminals) is about 5 mA.

Finally, the recommended minimum circuit currents of power supply are shown in Table 13 which takes into consideration ripple current and sufficient margins at the worst conditions, e.g. 5 times higher than the calculated value.

Table 13 The recommended minimum circuit current of power supply (Unit: [mA])

Item	The circuit current of +15 V control supply	The circuit current of +5 V logic supply
VDD ≤ 20 V, FSW ≤ 20 KHz	98.0	25.0

4.8 Recommended layout pattern

4.8.1 OCP & SCP function

It is recommended that the ITRIP filter capacitor connections to the IM828 pins be as short as possible. The ITRIP filter capacitor should be connected to the VSS pin directly without overlapped ground pattern. The signal ground and power ground should be as short as possible and connected at only one point via the filter capacitor of VDD line.

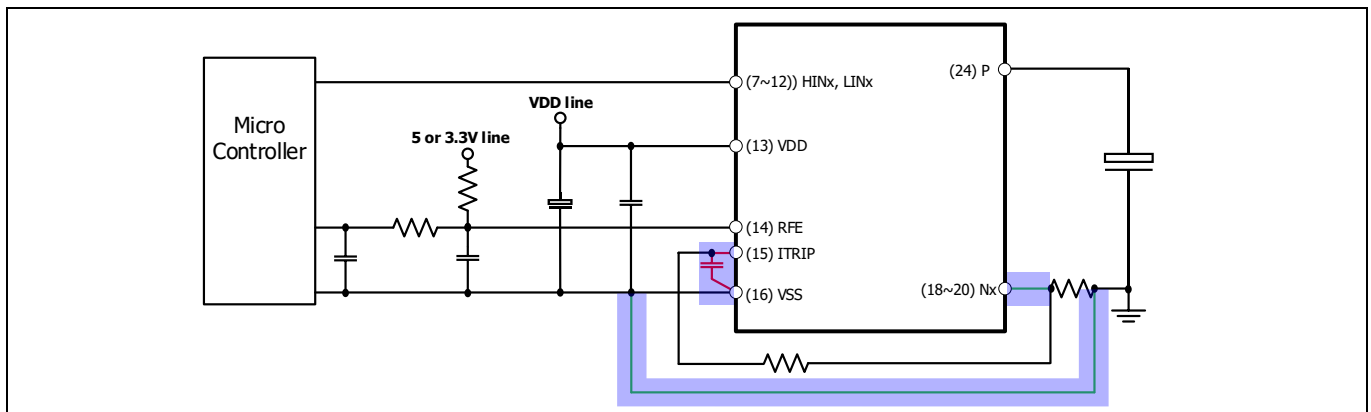


Figure 21 Recommended layout pattern for OCP & SCP function

4.8.2 Power line

Probably the most important parasitic components which have to be taken into account for the development of a power electronic application are the the stray inductance. Stray inductance is a consequence of internal and external connections between the semiconductor devices and the power electronic system. Figure 22 shows internal stray inductance by bonding wire, DCB pattern, and lead frame of IM828-XCC (approximately 250 [nH]) and example of external stray inductance between IM828-XCC and system board.

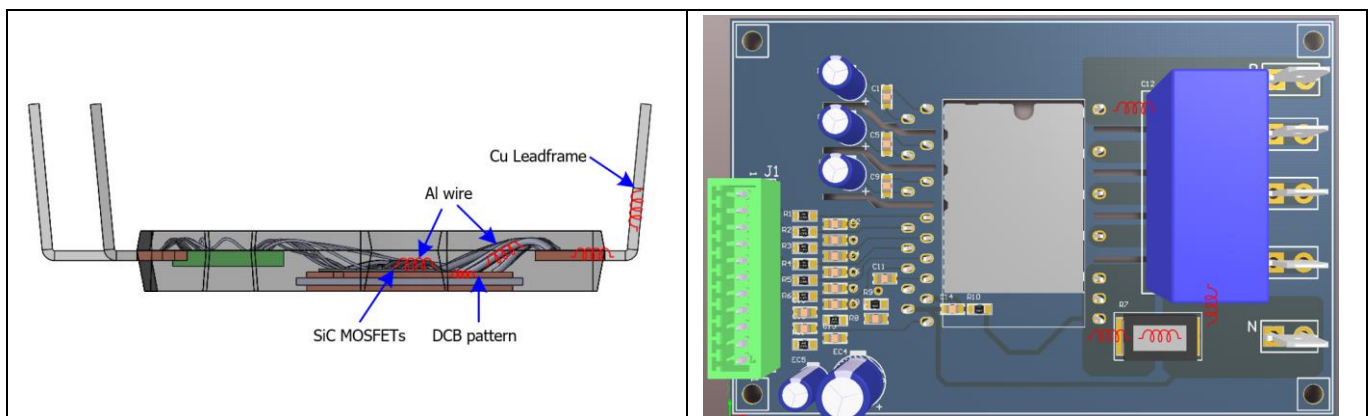


Figure 22 Internal stray inductance parameter (left) and possible external stray inductance parameters (right)

During a switching event a voltage drop across an inductor is calculated by the following equation.

$$\Delta V = L \times di/dt.$$

This voltage drop has influence on the turn-on and turn-off behavior of IM828-XCC. Figure 23 shows the turn-on and turn-off switching waveforms according to the stray inductance. The voltage drop during turn-on leads to a drop of V_{DS} leading to a reduction of the turn-on energy. During the turn-off of the device, the voltage leads to an increase of the voltage spike. If this voltage increase is larger than the device breakdown voltage the device will fail and the IPM will be destructed. Consequently the turn-off of a power device is the critical event to look at with respect to an IM828-XCC stray inductance. Table 14 shows switching characteristics with different stay inductance.

As CoolSiC™ 1200V MOSFET is much faster than Si IGBT within the same voltage class, SiC MOSFET with large stray inductance is limiting the use of SiC MOSFET with respect to the maximum allowed switching speed and/or applied voltages. However, IM828-XCC have relatively lower switching speeds (di/dt and dv/dt) for motor drive applications via optimized gate driver IC design. Therefore, IM828-XCC is relatively less affected by stray inductance. However, the turn-off switching speed of IM828-XCC is still much faster than Si IGBT IPM. So, larger stray inductance is able to induce larger voltage spikes as shown in Figure 23, which might cause device destruction. That is why users have to reduce the stray inductance as much as possible.

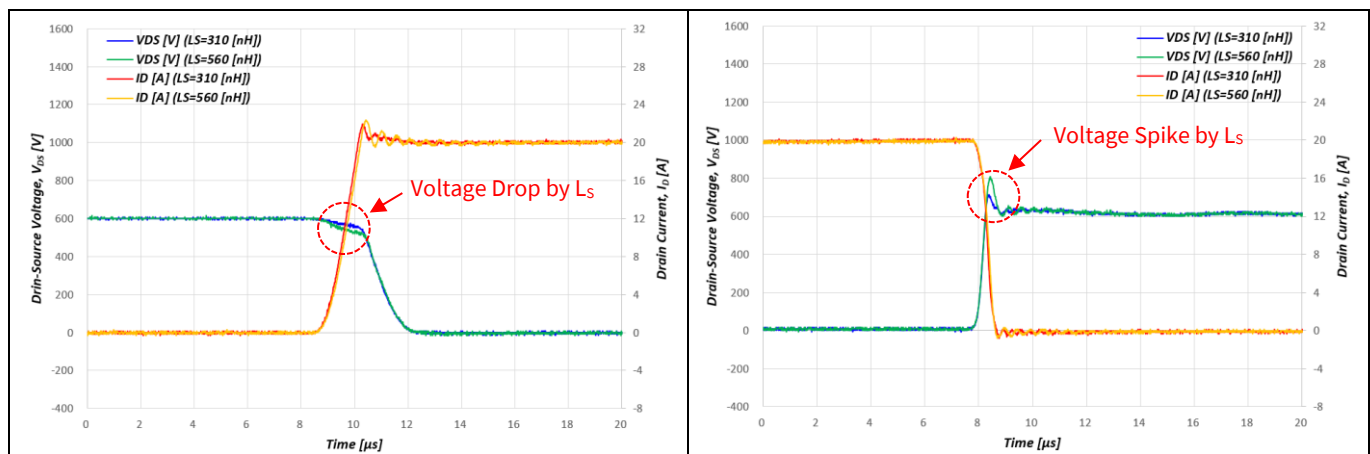


Figure 23 Turn-on(left) and Turn-off(right): Switching waveform comparison with different stray inductance, L_S ($V_{DC} = 600\text{ V}$, $V_{DD} = 15\text{ V}$, $I_D = 20\text{ A}$, $T_J = 25\text{ °C}$, inductive load = 3 mH)

Table 14 Switching characteristics with total(internal and external) stray inductance

	Total stray inductance, L_S [nH]	Slew rate, di/dt [A/ μ s]	Voltage drop, V_D [V]	Switching loss, E_{ON} [μ J]
Turn-on	310	152.4	47.6	1673.0
	560	142.9	80.0	1580.0
	Total stray inductance, L_S [nH]	Slew rate, di/dt [A/ μ s]	Voltage spike, V_S [V]	Switching loss, E_{OFF} [μ J]
Turn-off	310	333.2	112.0	296.0
	560	333.3	198.0	342.0

4.9 Recommended wiring of shunt resistor and snubber capacitor

External current sensing resistors are applied to detect overcurrent of phase currents. A long wiring pattern between the shunt resistors and IM828 will cause excessive surges that might damage the IM828's internal IC and current detection components. This may also distort the sensing signals. To decrease the pattern inductance, the wiring between the shunt resistors and IM828 should be as short as possible.

As shown in Figure 24 snubber capacitors should be installed in the right location so as to suppress surge voltages effectively. Generally a high frequency non-inductive capacitor of around $0.1 \sim 0.22 \mu\text{F}$ is recommended. If the snubber capacitor is installed in the wrong location '1' as shown in Figure 24, it cannot suppress the surge voltage effectively. If the capacitor is installed in location '2', the charging and discharging currents generated by wiring inductance and the snubber capacitor will appear on the shunt resistor. This will impact the current sensing signal and the SC protection level will be a little lower than the calculated design value. The "2" position surge suppression effect is greater than the location '1' or '3'. The '3' position is a reasonable compromise with better suppression than in location '1' without impacting the current sensing signal accuracy. For this reason, location '3' is generally used.

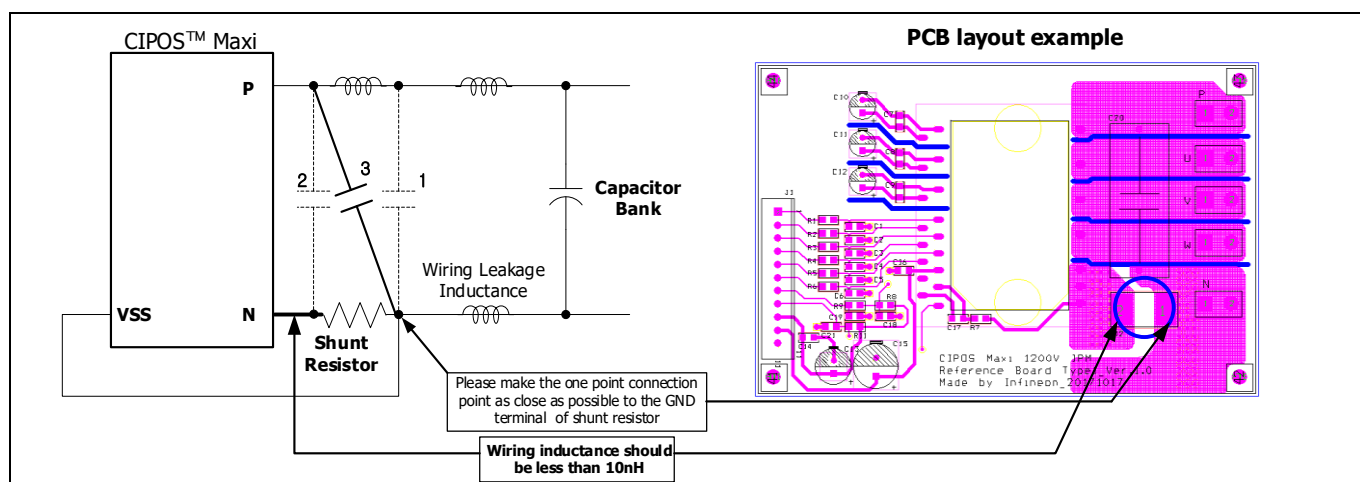


Figure 24 Recommended wiring of shunt resistor and snubber capacitor

4.10 Pin and screw hole coordinates for IM828 footprint

Figure 25 shows the IM828 position on the PCB to indicate center coordinates of each pin and screw hole in Table 15.

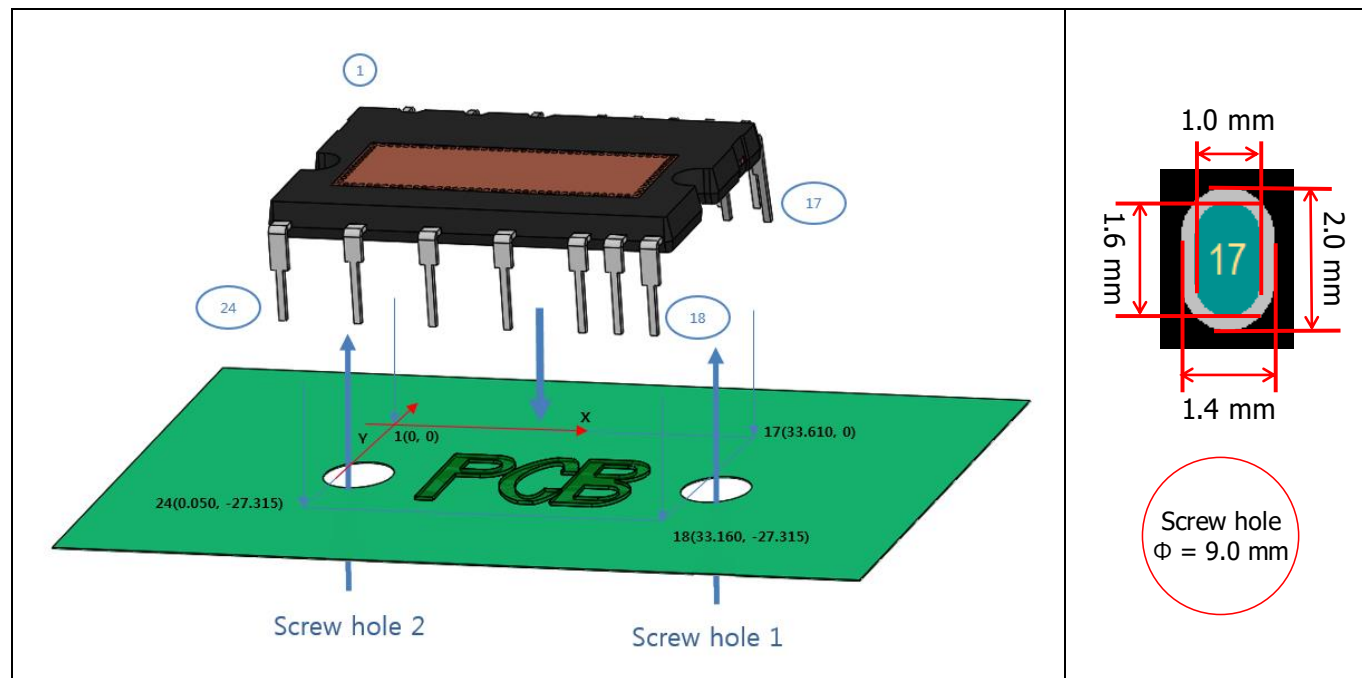


Figure 25 IM828 position on PCB (Unit: [mm]) and example of pad design(1~24pin)

Table 15 Pin & screw holes coordinates for IM828 footprint (Unit: [mm])

Pin Number		X	Y	Pin Number		X	Y
Signal Pin	1	0.000	0.000	Signal Pin	14	28.410	2.997
	2	1.600	2.997		15	30.010	0.000
	3	5.737	0.000		16	31.610	2.997
	4	7.337	2.997		17	33.610	0.000
	5	11.473	0.000	Power Pin	18	33.160	-27.315
	6	13.073	2.997		19	29.960	-27.315
	7	17.210	0.000		20	26.760	-27.315
	8	18.810	2.997		21	20.083	-27.315
	9	20.410	0.000		22	13.405	-27.315
	10	22.010	2.997		23	6.728	-27.315
	11	23.610	0.000		24	0.050	-27.315
	12	25.210	2.997	Screw Hole	1	33.355	-15.308
	13	26.810	0.000		2	-0.145	-15.308

5 Protection features

5.1 Undervoltage protection

Control and gate drive power for the IM828 is normally provided by a single 15 V supply that is connected to the module VDD and VSS terminals. For proper operation this voltage should be regulated to $15\text{ V} \pm 10\%$. Table 16 describes the behavior of the IM828 for various control supply voltages. The control supply should be well filtered with a low-impedance electrolytic capacitor and a high-frequency decoupling capacitor connected at the IM828's pins.

High-frequency noise on the supply might cause the internal control IC to malfunction and generate erroneous fault signals. To avoid these problems, the maximum ripple on the supply should be less than $\pm 1\text{ V}/\mu\text{s}$.

The potential at the module's VSS terminal is different from that at the N power terminal by the voltage drop across the sensing resistor. It is very important that all control circuits and power supplies be referred to this point and not to the N terminal. If circuits are improperly connected, the additional current flowing through the sense resistor might cause improper operation of the short-circuit protection function. In general, it is best practice to make the common reference (V_{SS}) a ground plane in the PCB layout.

The main control power supply is also connected to the bootstrap circuits to generate the floating supplies for the high-side gate drives.

When control supply voltage (V_{DD} and V_{BS}) falls down under UVLO (undervoltage lockout) level, MOSFETs will turn off while ignoring the input signal.

Table 16 IM828 functions versus control power supply voltage

Control Voltage Range [V]	Function operations
0 ~ 4	Control IC does not operate. Undervoltage lockout and fault output do not operate.
4 ~ 12.5	When the undervoltage lockout function is activated, control input signals are blocked and a fault-out signal (V_{RFE}) is generated.
12.5 ~ 13.5	MOSFETs will be operated in accordance with the control gate input. Driving voltage is below the recommended range, so the $V_{DS(on)}$ and the switching losses will be larger than under normal conditions. And high-side MOSFETs cannot operate after V_{BS} initial charging, because V_{BS} cannot reach V_{BSUV+} .
13.5 ~ 18.0 for V_{DD} 12.5 ~ 18.0 for V_{BS}	Normal operation. This is the recommended operating condition. V_{DD} of 15 V is recommended when only integrated bootstrap circuitry is used.
18.0 ~ 20 for V_{DD} , V_{BS}	MOSFETs are still operated. Because driving voltage is above the recommended range, MOSFETs' switching is faster. It causes increasing system noise. And peak short-circuit current might be too large for proper operation of the short-circuit protection.
Over 20	Control circuit in the IM828 might be damaged.

Protection features

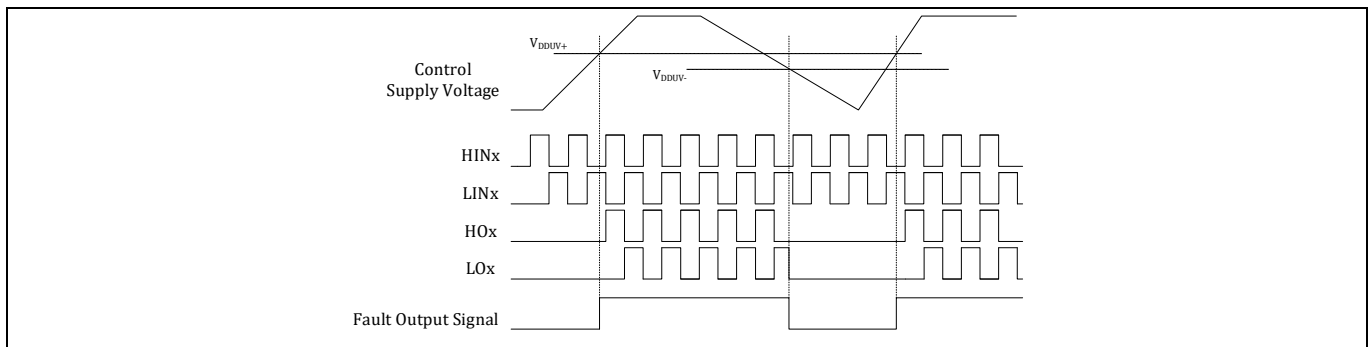


Figure 26 Timing chart of low-side undervoltage protection function

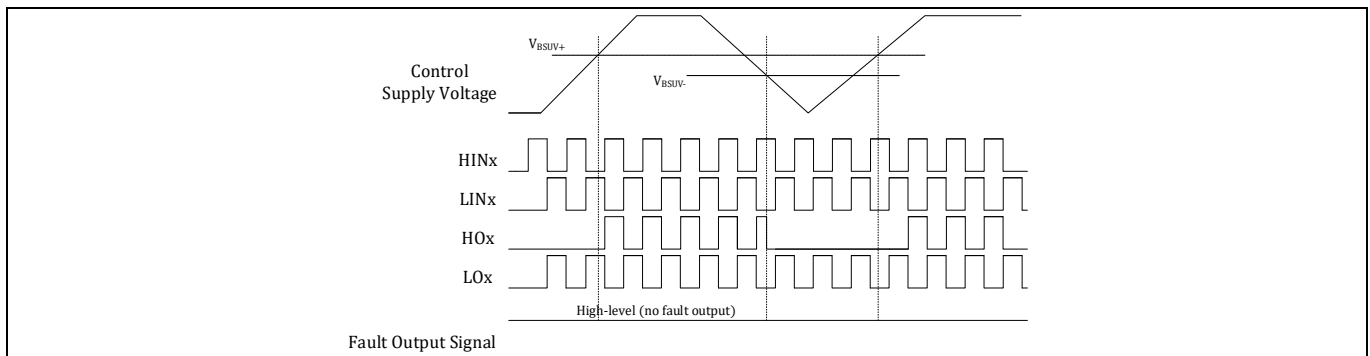


Figure 27 Timing chart of high-side undervoltage protection function

5.2 Overcurrent protection

5.2.1 Timing chart of overcurrent (OC) protection

The IM828 has an overcurrent shutdown function. Its internal IC monitors the voltage of the ITRIP pin, and if this voltage exceeds the $V_{IT,TH+}$, which is specified in the device's datasheets, a fault signal is activated and all MOSFETs are turned off. Typically the maximum short-circuit current magnitude is gate-voltage dependant. A higher gate voltage results in a larger short-circuit current. In order to avoid this potential problem, the maximum overcurrent trip level is usually set to below 2 times the nominal rated collector current. The overcurrent protection-timing chart is shown in Figure 28.

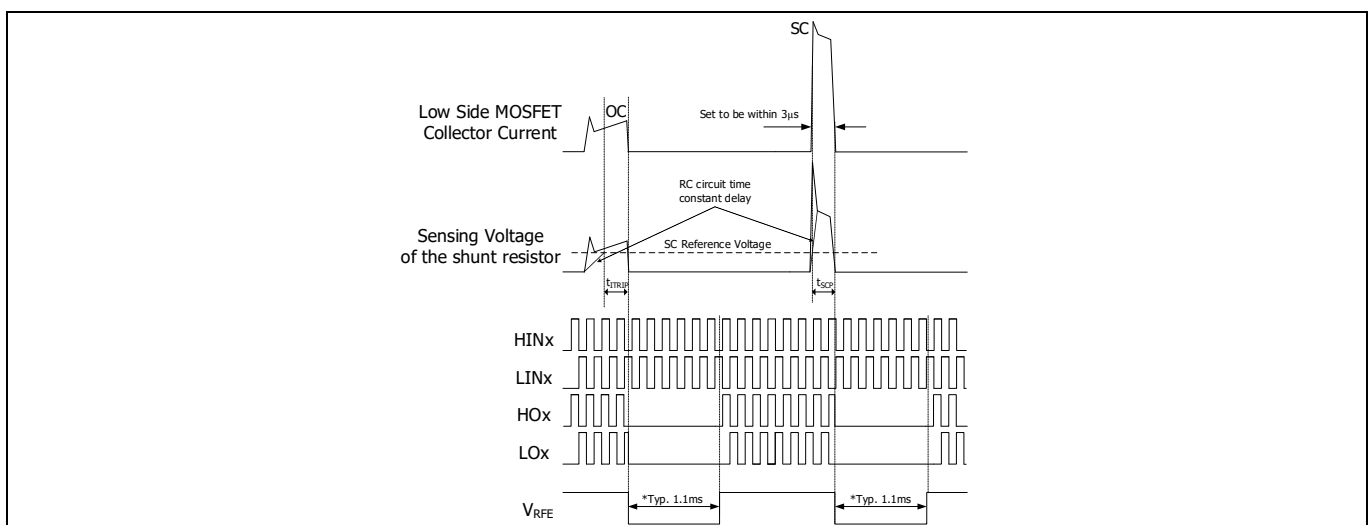


Figure 28 Timing chart of overcurrent protection function

(* $t_{FLT,CLR}$ is defined by R_{RCIN} , C_{RCIN} , please refer to Section 5.3)

Protection features

5.2.2 Selecting current sensing shunt resistor

The value of the current sensing resistor is calculated by the following expression:

$$R_{SH} = \frac{V_{IT,TH+}}{I_{OC}} \quad (1)$$

Where $V_{IT,TH+}$ is the ITRIP positive-going threshold voltage of IM828. It is typically 0.5 V. I_{OC} is the current of OC detection level.

The maximum value of OC protection level should be set lower than the repetitive peak collector current in the datasheet taking into consideration the tolerance of the shunt resistor. For example, the maximum peak collector current of IM828-XCC is 50 A_{peak}, and thus, the recommended value of the shunt resistor is calculated as

$$R_{SH(min)} = \frac{0.5}{50} = 0.01 \Omega$$

For the power rating of the shunt resistor, the following list should be considered:

- Maximum load current of inverter (I_{rms})
- Shunt resistor value at $T_c = 25^\circ\text{C}$ (R_{SH})
- Power derating ratio of shunt resistor at $T_{SH}=100^\circ\text{C}$ according to the manufacturer's datasheet
- Safety margin

The shunt resistor power rating is calculated by the following equation.

$$P_{SH} = \frac{I_{rms}^2 \times R_{SH} \times \text{margin}}{\text{derating ratio}} \quad (2)$$

For example, in the case of IM828-XCC and $R_{SH} = 10 \text{ m}\Omega$ (WSR5R0100F: Vishay)

- Max. load current of the inverter : 14 A_{rms}
- Power derating ratio of shunt resistor at $T_{SH}=100^\circ\text{C}$: 80%
- Safety margin : 30%

$$P_{SH} = \frac{14^2 \times 0.01 \times 1.3}{0.80} \approx 3.2 \text{ W}$$

A proper power rating of shunt resistor exceeds 3.2 W, e.g. 5 W. In addition, we recommend an SMD-type shunt resistor in order to minimize surge voltage by stray inductance of shunt resistor.

Model	Power rating [W]	Short time overload	Inductance [nH]	TCR [ppm/°C]	Operating temp. range [°C]
WSR5	5.0 at 70°C	3x rated power for 5 s	0.5 ~ 5.0	< 20	-55 ~ 150

Based on the previous equations, conditions, and calculation method, the minimum shunt resistance and resistor power of IM828 products have been introduced, and are listed in Table 17. It is noted that a proper resistance and power rating higher than the minimum value should be chosen considering the overcurrent protection level required in the application.

Table 17 Minimum R_{SH} and P_{SH}

Product	Max. peak current	Min. shunt resistance, R_{SH}	Min. shunt resistor power, P_{SH}
IM828-XCC	50 A	10 mΩ	5.0 W

Protection features

5.2.3 Delay time

The RC filter is necessary in the overcurrent sensing circuit to prevent malfunction of OC protection caused by noise. The RC time constant is determined by considering the noise duration and the short-circuit withstand time capability of the MOSFET.

When the sensing voltage on the shunt resistor exceeds the ITRIP positive-going threshold ($V_{IT,TH+}$), this voltage is applied to the ITRIP pin of the IPM via the RC filter. Table 18 shows the specification of the OC protection reference level. The filter delay time (t_{Filter}) until that the input voltage of ITRIP pin rises to the ITRIP positive threshold voltage is defined by the following equation (3), (4).

$$V_{IT,TH+} = R_{SH} \cdot I_C \cdot \left(1 - \frac{1}{e^{\frac{t_{Filter}}{\tau}}}\right) \quad (3)$$

$$t_{Filter} = -\tau \cdot \ln\left(1 - \frac{V_{IT,TH+}}{R_{SH} \cdot I_C}\right) \quad (4)$$

Where, $V_{IT,TH+}$ is the ITRIP pin input voltage, I_C is the peak current, R_{SH} is the shunt resistor value and τ is the RC time constant. In addition there is a short-circuit propagation delay time of Itrip (t_{SCP}) which is defined by the propagation delay time from $V_{IT,TH+}$ to 10% of I_{SC} . Please refer to Table 19.

Table 18 Specification of OC protection reference level $V_{IT,TH+}$

Item	Symbol	Min.	Typ.	Max.	Unit
ITRIP positive-going threshold	$V_{IT,TH+}$	0.475	0.500	0.525	V

Table 19 Shut-down propagation delay

Item	Condition	Min.	Typ.	Max.	Unit
Short-circuit propagation delay time (t_{SCP})	IM828-XCC From $V_{IT,TH+}$ to 10% I_{SC}	-	1200	-	ns

Therefore, the total time from ITRIP positive-going threshold ($V_{IT,TH+}$) to the shut-down of the MOSFET becomes:

$$t_{total} = t_{Filter} + t_{SCP}$$

The short-circuit propagation delay can be changed by operating conditions such as operating temperature and V_{DD} , V_{DC} . The total delay must be less than the 3 μ s of short-circuit withstand time (t_{SC}) in the datasheet. Thus, the RC time constant should be set in the range of 1 ~ 2 μ s. However, the practical RC time constant value is 1 ~ 2 μ s, so recommended values for the filter components are $R7 = 1.8 \text{ k}\Omega$ and $C17 = 1 \text{ nF}$.

5.3 RFE circuit

The RFE pin combines three functions in one pin: fault output, enable input, and RC-network-based programmable fault clear timing.

The RFE pin is normally connected to an RC network on the application circuit in Figure 29. Under normal operating conditions, R_{RCIN} pulls the RFE pin to 5 V, thus enabling all the functions in the IPM. The microcontroller can pull this pin low to disable the IPM functionality. This is the Enable function.

Protection features

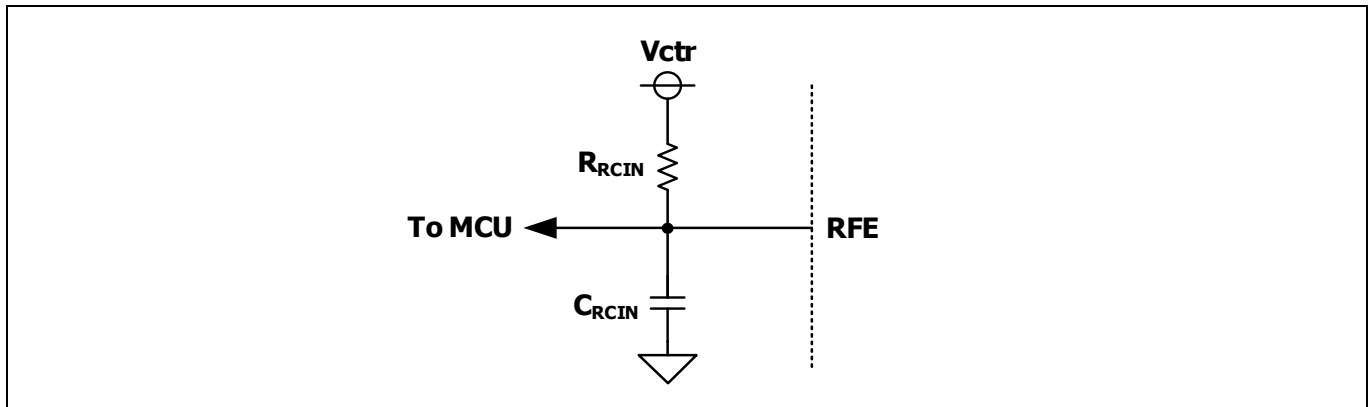


Figure 29 Typical application circuit for RFE pin

The fault-out function allows the IM828 to report a fault event to the MCU by pulling the RFE pin low in one of two situations. The first is an undervoltage condition on V_{DD} and the second is when the ITRIP pin detects a voltage rising above $V_{RFE,TH+}$.

The programmable fault-clear timing function provides a means of automatically re-enabling the IPM operation a preset amount of time ($T_{FLT,CLR}$) after the fault event has disappeared. Figure 30 shows the RFE-related circuit block diagram inside the IM828.

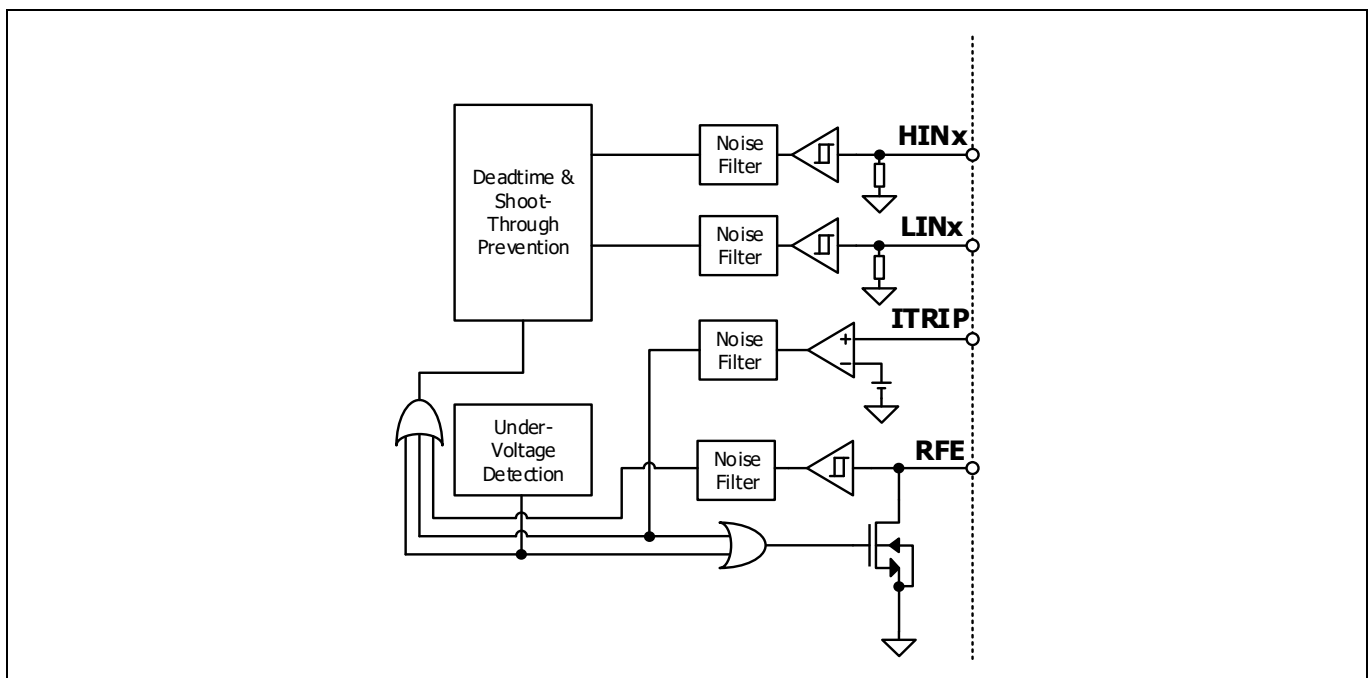


Figure 30 RFE internal circuit diagram

The length of total $T_{FLT,CLR}$ can be determined by using the formula below.

$$RFE(t) = V_{ctr} \times \left(1 - e^{-\frac{t}{RC}}\right)$$

$$Total\ T_{FLT,CLR} = -R_{RCIN} \times C_{RCIN} \times \ln\left(1 - \frac{V_{RFE,TH+}}{V_{ctr}}\right) + \text{Internal fault-clear time } (T_{FLT,CLR})$$

For example, if V_{ctr} is 5.0 V, R_{RCIN} is 1 M Ω , and C_{RCIN} is 2 nF,

$$Total\ T_{FLT,CLR} = -1\ M\Omega \times 2\ nF \times \ln\left(1 - \frac{1.9\ V}{5.0\ V}\right) + 160\ \mu s \cong 1.1\ ms$$

Protection features

Table 20 Examples of total $t_{FLT,CLR}$

V_{CTR} [V]	R_{RCIN} [M Ω]	C_{RCIN} [nF]	Total $T_{FLT,CLR}$ [ms]	V_{CTR} [V]	R_{RCIN} [M Ω]	C_{RCIN} [nF]	Total $T_{FLT,CLR}$ [ms]
3.3	2.0	1.0	1.9	5.0	2.0	1.0	1.1
	1.0	1.0	1.0		1.0	1.0	0.6
	0.5	1.0	0.6		0.5	1.0	0.4
	2.0	2.0	3.6		2.0	2.0	2.1
	1.0	2.0	1.9		1.0	2.0	1.1
	0.5	2.0	1.0		0.5	2.0	0.6

Table 21 RFE maximum rating

Item	Symbol	Condition	Rating	Unit
RFE voltage	V_{RFE}	Applied between RFE-VSS	$-1 \sim V_{DD} + 0.3$	V

Table 22 Electric characteristics

Item	Symbol	Condition	Min.	Typ.	Max.	Unit
RFE output voltage	V_{RFE}	$I_{RFE} = 10 \text{ mA}$, $V_{ITRIP} = 1 \text{ V}$	-	0.7	-	V
RFE MOSFET Resistance	$R_{ON,RFE}$	-	-	40	70	Ω
RFE positive-going threshold	$V_{RFE,TH+}$	-	-	1.9	2.3	V
RFE negative-going threshold	$V_{RFE,TH-}$	-	0.7	0.9	-	V

Because the RFE terminal is an open-drain type, it must be pulled up to the high level via a pull-up resistor. The resistor has to be calculated according to the above specifications.

5.4 Sleep function

The sleep function is activated after each trigger of ITRIP or undervoltage lockout. A new edge of each individual control signal LINx and HINx for activation of the outputs LOx or HOx is mandatory after release of signal RFE (fault out function). Please refer to Figure 31 for the description of the timing diagram.

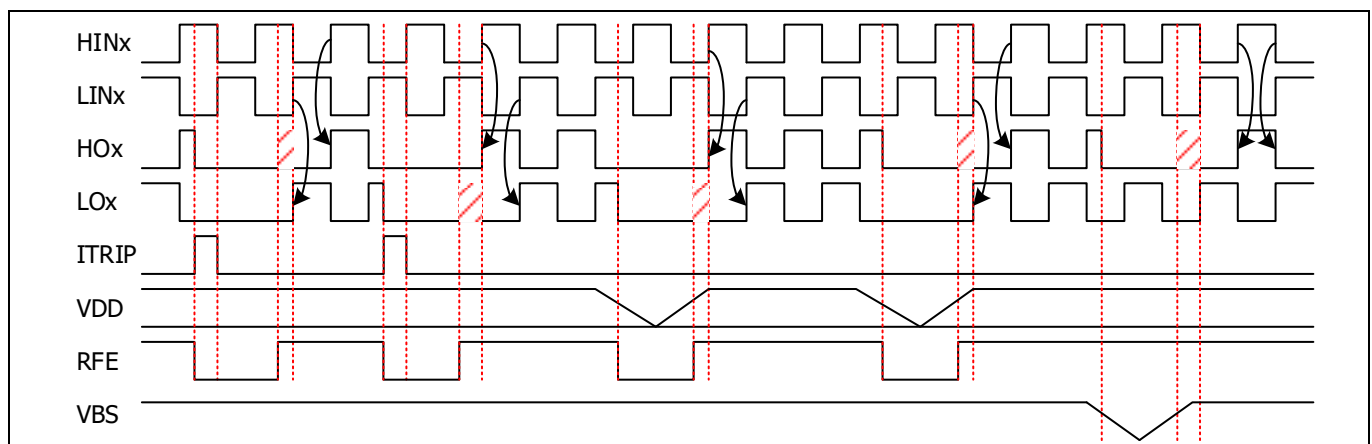


Figure 31 Sleep-function timing diagram ITRIP and UVLO

Protection features

5.5 Temperature monitor and thermal protection

The IM828 have independent pins for internal thermistors (85 kΩ at 25°C). The built-in thermistor is directly connected to the VSS internally. The typical application circuit looks like Figure 33. An external pull-up resistor connected to V_{ctr} ensures that the resulting voltage can be directly connected to the MCU.

In this reference board, the pull-up resistor is set to 18 kΩ so that the VTH voltage becomes 1.15 V and 0.75 V respectively for 5 V and 3.3 V control voltage (V_{ctr}) when the thermistor temperature is 100°C, as shown in Figure 34.

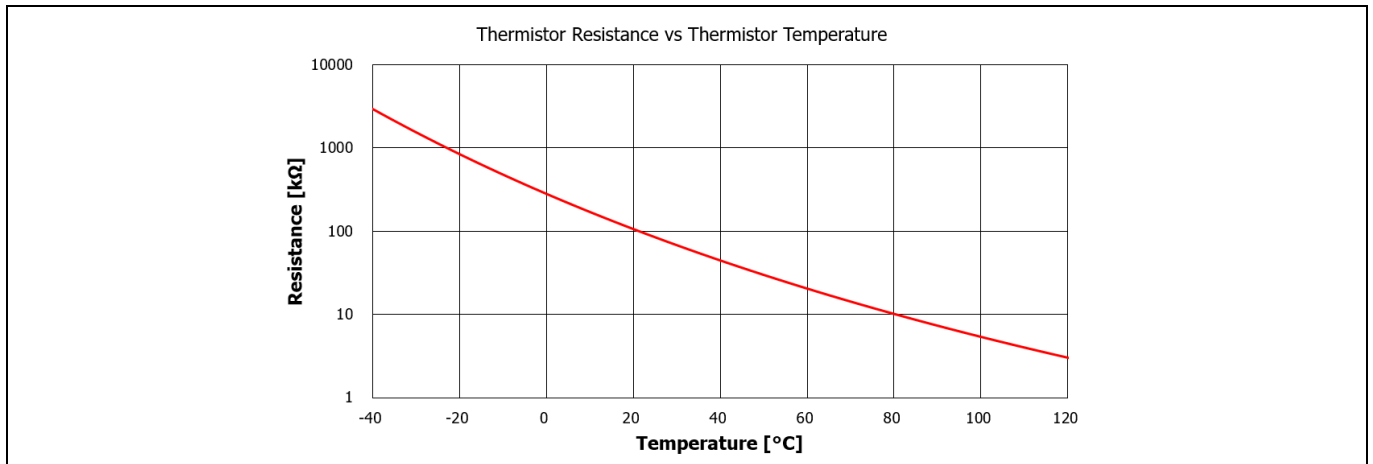


Figure 32 Internal thermistor resistance characteristics as a function of thermistor temperature

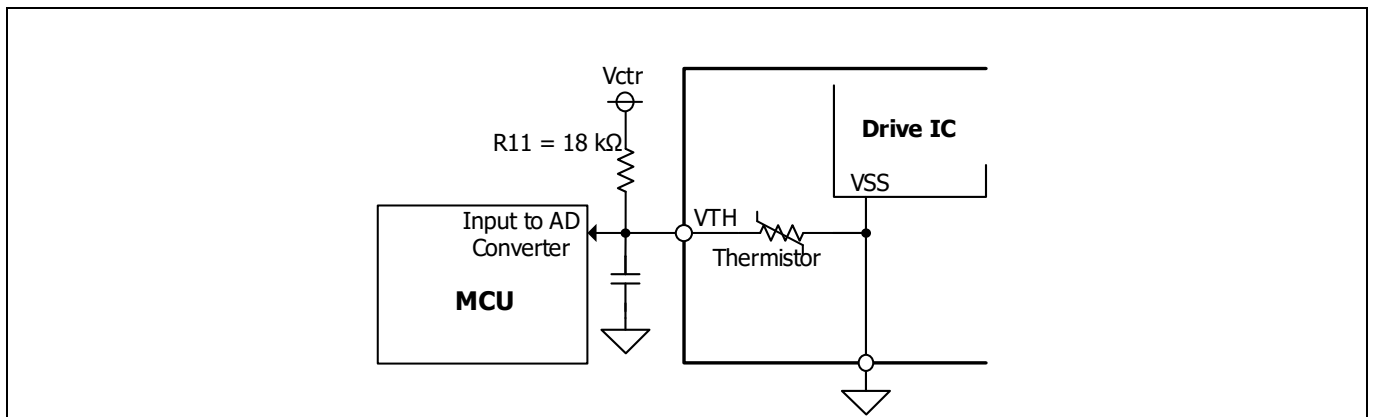


Figure 33 Circuit proposals for overtemperature protection

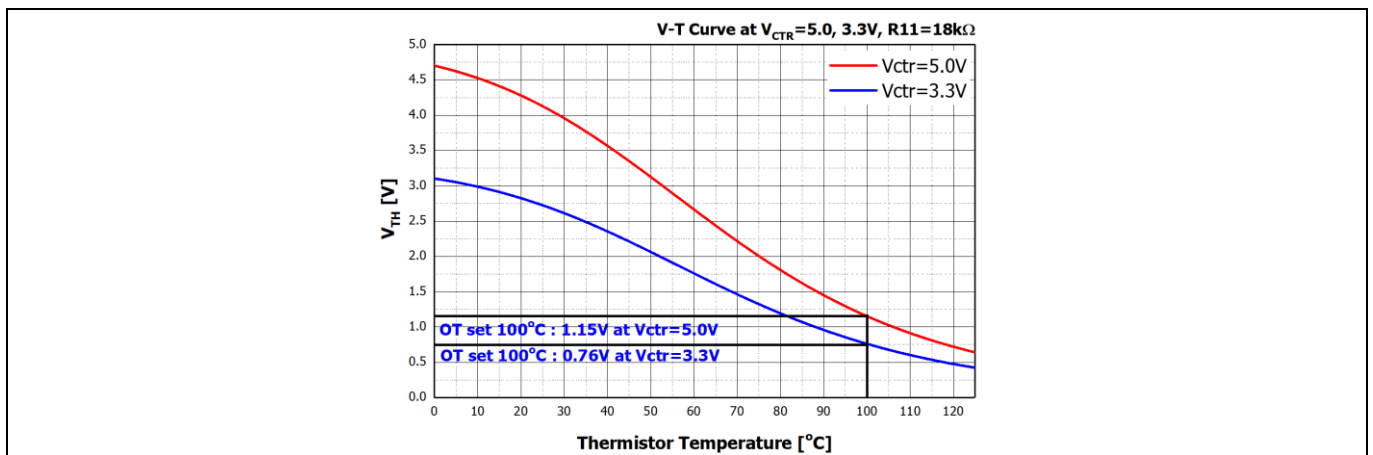


Figure 34 Voltage of VTH pin according to thermistor temperature

Protection features

The NTC thermistor is located on the inner PCB of the IPM as in Figure 35(a). So, thermistor temperature can not reflect power chip temperature directly. When the IPM is operated, the heat of power devices is transferred to the thermistor through the heat sink and package as seen in Figure 35(b).

Figure 36 shows the relationship between $T_{J(MEA)}$ (SiC MOSFET's maximum junction temperature), $T_{J(EST)}$ (estimated value by simulation), T_C (IPM case temperature), and T_{NTC} (thermistor temperature) under given conditions. However, this relationship is just one of example, as the relationship depends on the system conditions such as heat sink size, cooling system, control scheme, etc. Therefore, if the user would like to know the relationship between $T_{J(MEA)}$, $T_{J(EST)}$, T_C , and T_{NTC} on their system, we strongly recommend that they define the relationship by themselves with their own system.

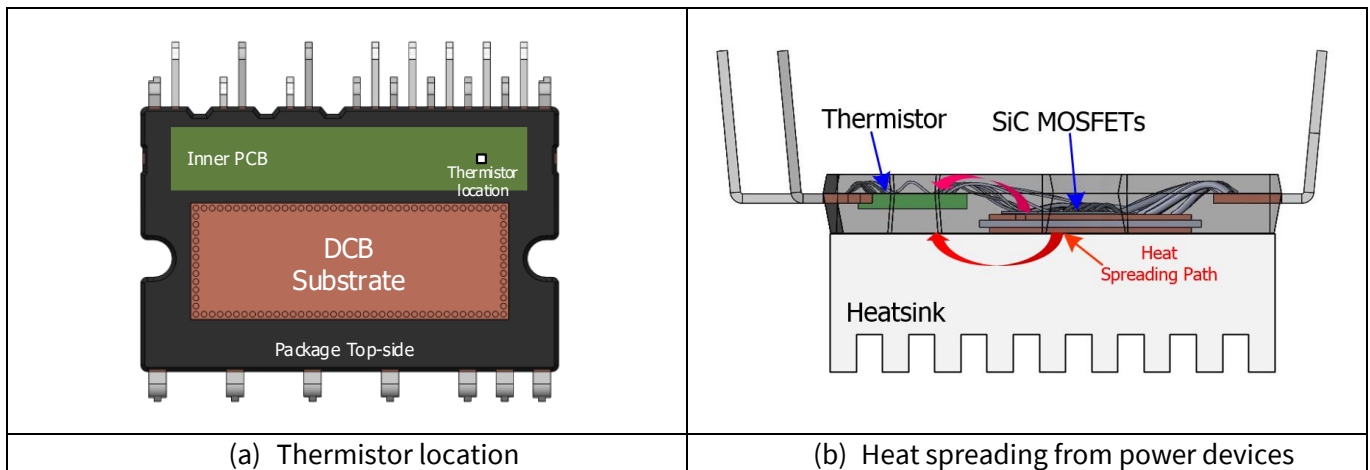


Figure 35 Thermistor location and heat spreading from power devices

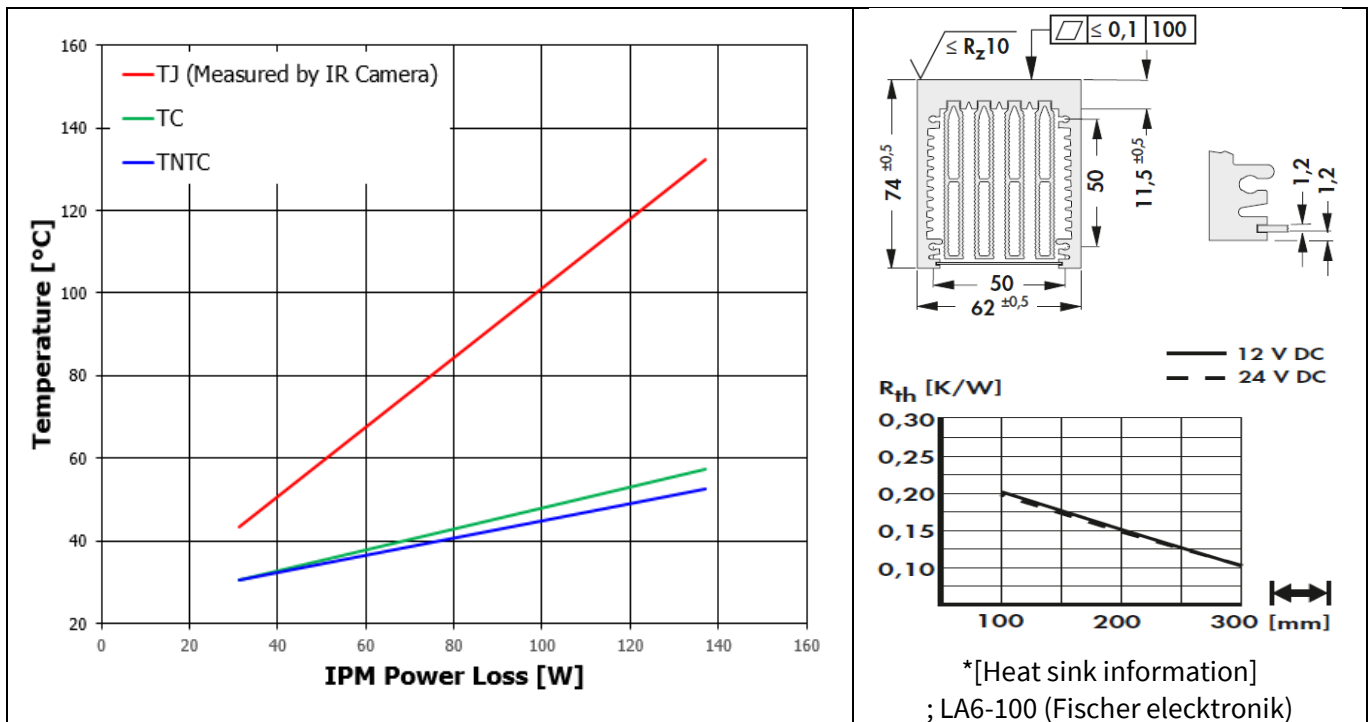


Figure 36 Example of relationship between $T_{J(MEA)}$, $T_{J(EST)}$, T_C , and T_{NTC} (Test conditions: $V_{DC} = 600$ V, $V_{DD} = 15$ V, $I_o = 5 \sim 20$ Apeak, $F_{SW} = 20$ kHz, $F_o = 3$ Hz, SVPWM, force cooling with *heat sink and fan, T_J is measured by Infrared camera, T_C measurement point refer to Figure 4)

Bootstrap circuit

6 Bootstrap circuit

6.1 Bootstrap circuit operation

The V_{BS} voltage, which is the voltage difference between $V_{B(U,V,W)}$ and $V_{S(U,V,W)}$, provides the supply to the high-side gate driver IC within the IM828. This supply voltage (V_{BS}) is recommended to be in the range of 12.5 ~ 18.5 V to ensure that the gate driver IC can fully drive the high-side MOSFET. The IM828 includes an undervoltage detection function for the V_{BS} to ensure that the IC does not drive the high-side MOSFET if the V_{BS} voltage drops below a specified voltage (refer to the datasheet). This function prevents the MOSFET from operating in a high dissipation mode. Please note here that the undervoltage lockout function of any high-side section acts only on the triggered channel without any feedback to the control level.

There are a number of ways in which the V_{BS} floating supply can be generated. One of them is the bootstrap method described here. This method has the advantage of being simple and cheap. However, the duty cycle and on-time are limited by the requirement to refresh the charge in the bootstrap capacitor. The bootstrap supply is formed by a combination of a diode (D_{BS}), resistor (R_{BS}) and capacitor (C_{BS}) as shown in Figure 39 (a). The current flow path of the bootstrap circuit is shown in Figure 39 (a). When V_S is pulled down to ground (either through the low side or the load), the bootstrap capacitor (C_{BS}) is charged through the bootstrap diode (D_{BS}) and the resistor (R_{BS}) from the V_{DD} supply.

6.2 Internal bootstrap functionality characteristics

The IM828 includes three bootstrap functionalities in the internal gate driver IC, which consist of three diodes and three resistors, as shown in Figure 3. A typical value of the internal bootstrap resistor is 120 Ω at room temperature. For more information, please refer to Figure 37 and Table 23.

V_{DD} of 15 V is recommended when only the integrated bootstrap circuitry is used.

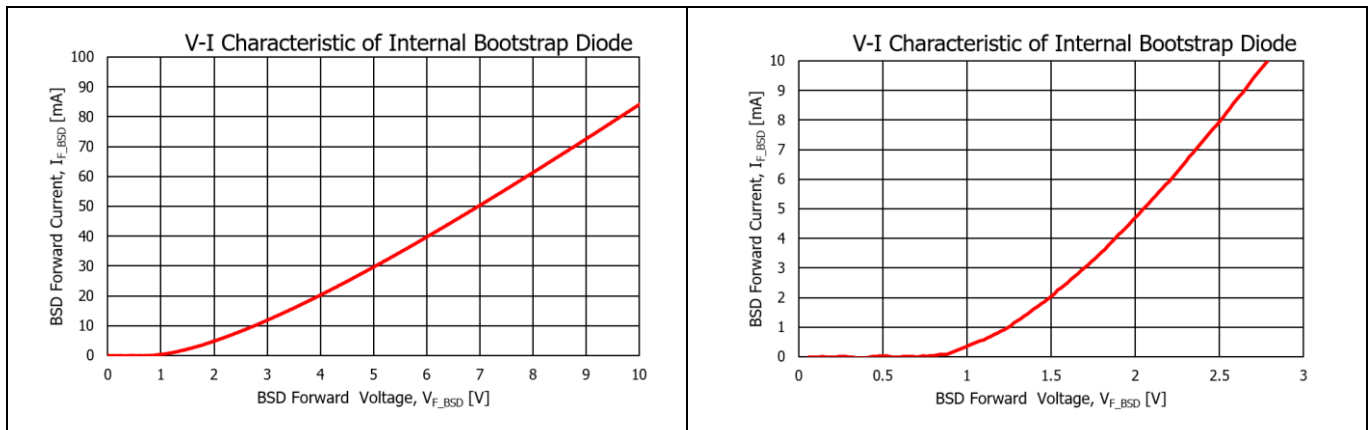


Figure 37 Internal bootstrap diode I_F - V_F characteristics

Table 23 Electrical characteristics of internal bootstrap parameters

Description	Condition	Symbol	Value			Unit
			Min.	Typ.	Max.	
Repetitive peak-reverse voltage		V_{RRM}	1200	-	-	V
Diode resistance	Between $V_F = 4$ V and $V_F = 5$ V	R_{BSD}	-	120	-	Ω
Diode forward voltage	$I_F = 0.3$ mA	V_{F_BSD}	-	0.9	-	V

Bootstrap circuit

6.3 Initial charging of bootstrap capacitor

Once we assume that the use one-pulse charging method is used, the time required for initial charge depends on capacitance of C_{BS} , forward voltage of bootstrap diode (V_{F_BSD}) and resistance of R_{BS} . Charge is performed with a time constant that is roughly calculated from capacitance of C_{BS} and resistance of R_{BS} .

Example of calculation charging waveform is shown in Figure 38.

Conditions : CIPOS™ Maxi IM828-XCC (1200 V / 20 A, D_{BS} and R_{BS} (120 Ω) are embedded on gate driver IC), C_{BS} = 22 μ F / 100 μ F, V_{DD} = 15 V and R_{SHUNT} = 10 m Ω .

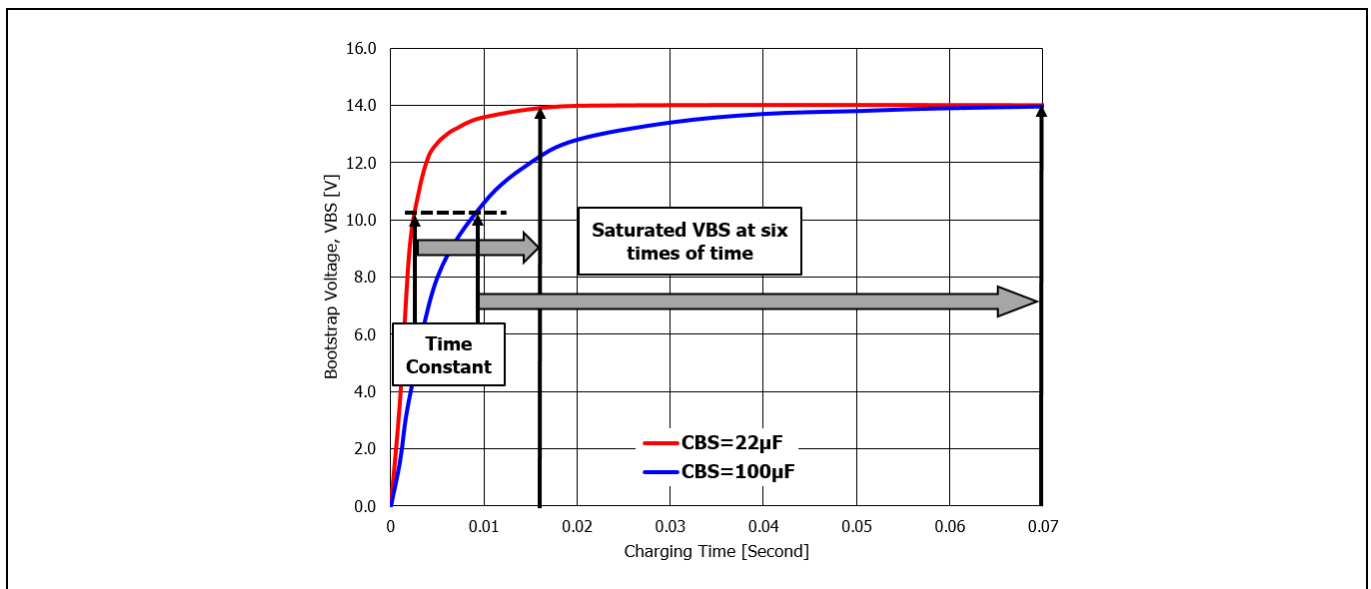


Figure 38 Bootstrap circuit operation and initial changing

As in the above figure, V_{BS} does not reach target voltage (about 70%) by charging up to time constant (e.g. $= C \times R = 22 \mu\text{F} \times 120 \Omega = 2.64 \text{ ms}$). To reach target voltage, approximately six times the time constant will be needed. Target voltage does not reach the V_{DD} . It will become 1.0 V lower than the control supply voltage due to voltage drop of low-side MOSFET ($V_{DS(ON)}$) and D_{BS} (V_F) which are in charging path. Refer to Figure 39(a).

Initial charging needs to be performed until V_{BS} (voltage of C_{BS}) exceeds recommended minimum bootstrap voltage (V_{BS_min}) 12.5 V. (It is recommended to charge as high as possible with consideration for voltage drop between the end of charging and start of inverter operation.)

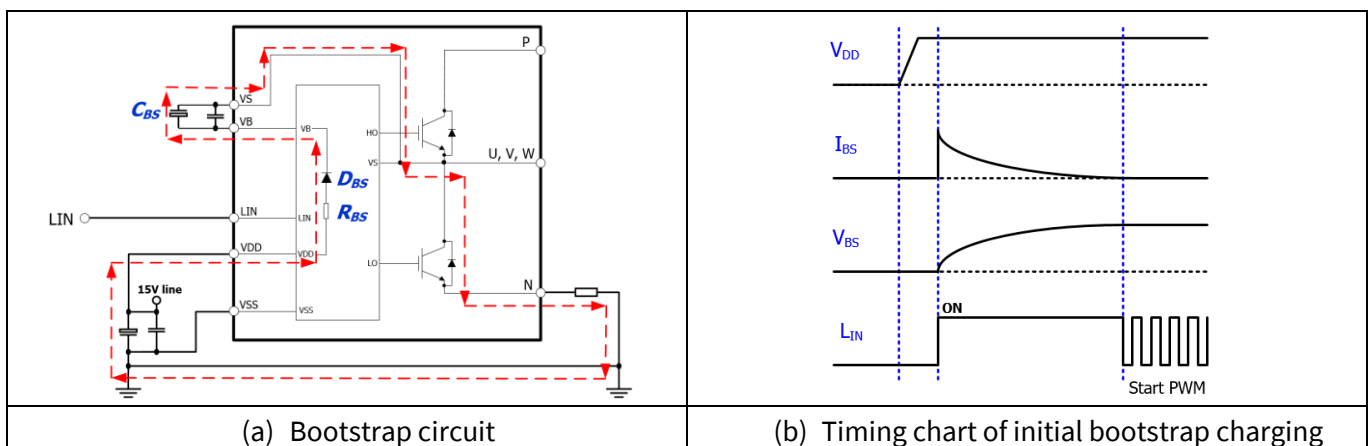


Figure 39 Bootstrap circuit operation and initial changing

Bootstrap circuit

6.4 Bootstrap supply circuit current at switching mode

Bootstrap supply circuit current at steady state, I_{QBS} (quiescent V_{BS} supply current) is typical 175 μ A. But at switching mode, because gate charge and discharge are repeated by switching event, the circuit current (I_{BS}) can exceed I_{QBS} and increases proportional to switching frequency (F_{SW}). For reference, Figure 40 shows typical I_{BS} vs F_{SW} characteristics for IM828-XCC. (Conditions: $V_{DD} = V_{BS} = 15$ V, $T_J = 150^\circ$ C, MOSFET ON duty = 50%)

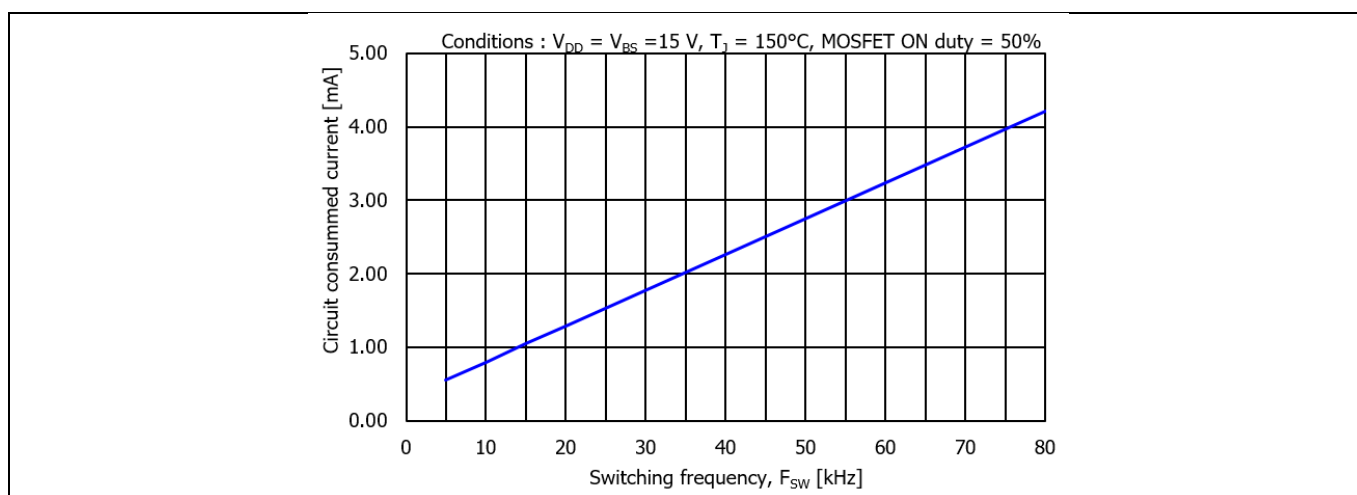


Figure 40 Bootstrap circuit consumed current (I_{BS}) vs. switching frequency (F_{SW}) for IM828-XCC

6.5 Bootstrap circuit design

When IM828-XCC for bootstrap circuit is designed, it is necessary to consider various conditions such as temperature characteristics, change by lifetime, variation and so on. Notes for designing these devices are listed as below. For more detailed information about driving via the bootstrap circuit, please refer to the application note “AN2020-14_Bootstrap circuit design for CIPOS™ IPM”.

6.5.1 Bootstrap capacitor

Electrolytic capacitors are used for C_{BS} generally. And recently MLCC (multilayer ceramic capacitor) with large capacitance are also applied. But, the DC bias characteristics of the MLCC when applying DC voltage are considerably different from that of the electrolytic capacitor, especially the large capacitance type. Some differences in capacitance characteristics between electrolytic and ceramic capacitors are listed in Table 24.

Table 24 Difference of capacitance characteristics between electrolytic and ceramic capacitors

	Electrolytic capacitor	MLCC
Temperature characteristics (T_A : -20 ~ 85°C)	<ul style="list-style-type: none"> - Aluminum type: Low temp.: -10%, High temp.: +10% - Conductive polymer aluminum solide type: Low temp.: -5%, High temp.: +10% 	<ul style="list-style-type: none"> - Difference due to temp. characteristics: Low temp.: -5% ~ 0% High temp.: -5% ~ -10% (with X5R, X7R)
DC bias characteristics (applying DC15V)	Nothing within rating volage	<ul style="list-style-type: none"> Difference due to temp. characteristics, rating voltage, package size and so on -50% ~ -15% (with X7R, 50 VDC rating)

Bootstrap circuit

6.5.2 Bootstrap voltage variance under inverter operating conditions

When a bootstrap circuit is designed, bootstrap voltage (V_{BS}) variance needs to be considered at inverter operating conditions such as output current & frequency, switching frequency, modulation scheme, voltage ripple of V_{BS} and so on. Because lower bootstrap voltage can lead to high dissipation of high-side MOSFET or undervoltage lockout (UVLO) protection mode. Figure 41 shows trend of bootstrap voltage variance under given conditions based on simulation.

- Conditions: $V_{DC} = 600\text{ V}$, $V_{DD} = 15\text{ V}$, $I_o = 20\text{ A peak}$, SVPWM, ΔV_{BS} (Voltage ripple) $< 2.0\text{ V}$, $T_c = 25^\circ\text{C}$,

(a) $C_{BS} = 22\text{ }\mu\text{F}$, $F_{SW} = 20\text{ kHz}$, (b) $C_{BS} = 22\text{ }\mu\text{F}$, $F_o = 5\text{ Hz}$, (c) $F_{SW} = 20\text{ kHz}$, $F_o = 5\text{ Hz}$

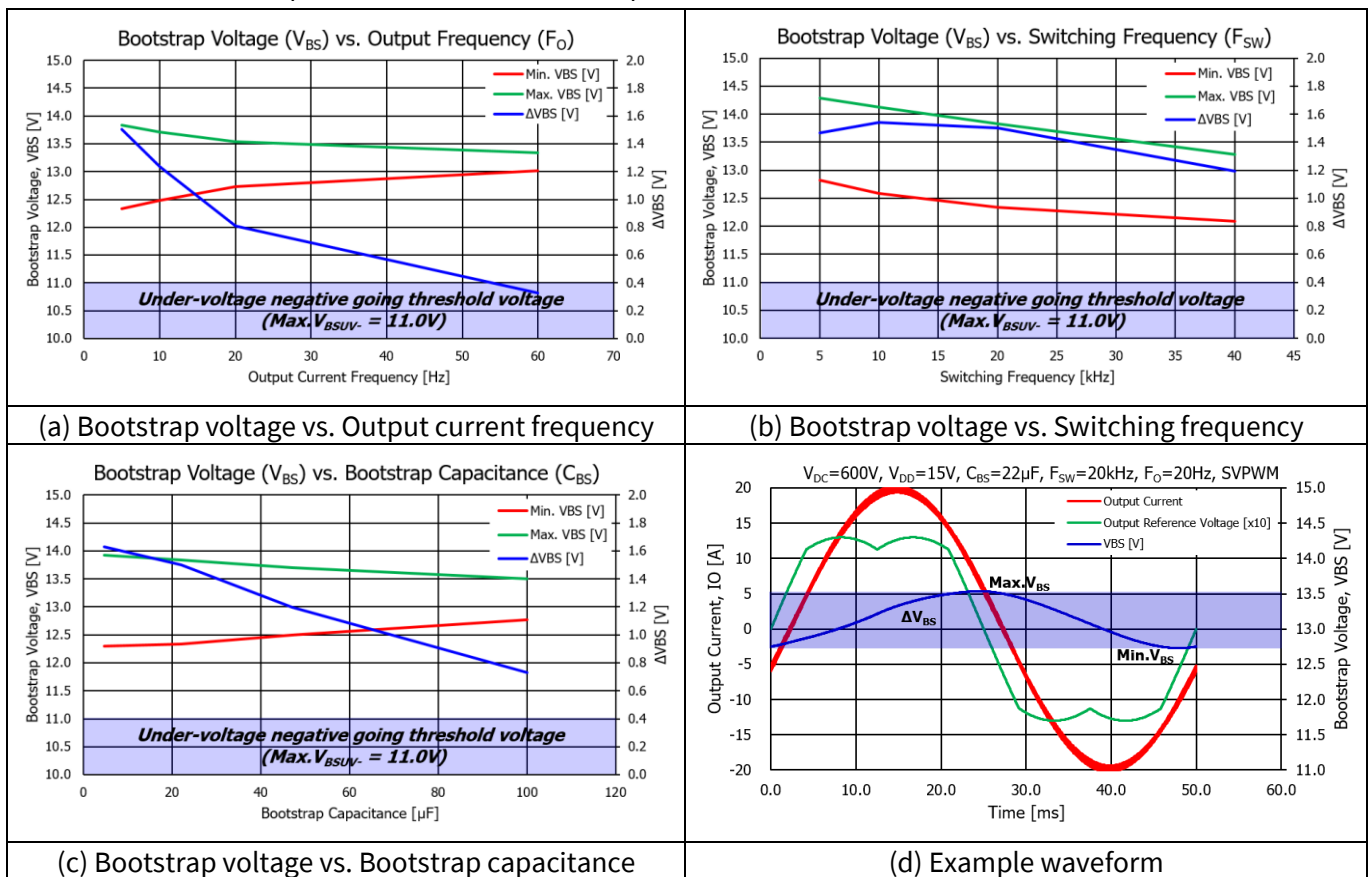


Figure 41 Bootstrap voltage (V_{BS}) variance under inverter operating conditions

According to Figure 41, except bootstrap capacitance (C_{BS}), major affected operating conditions to bootstrap voltage (V_{BS}) are

- Output current frequency, F_o
- Switching frequency, F_{SW}

Note that these results are only an example. It is necessary to consider enough confirmation and evaluation at the system design. Because bootstrap voltage is also affected by other operating conditions such as PWM scheme (e.g. discontinuous space vector PWM), power factor, modulation index, power switches (IGBT and MOSFET), and so on.

7 Thermal system design

7.1 Introduction

The thermal design of a system is a key issue of IM828 included in electronic systems such as drives. In order to avoid overheating and/or to increase the reliability, two design criteria are of importance:

- Low power losses
- Low thermal resistance from junction to ambient

The first criterion is already fulfilled when choosing IM828 as an intelligent power module for the application. To get the most out of the system, a proper heat sink choice is necessary. A good thermal design either allows the designer to maximize the power or to increase the reliability of the system (by reducing the maximum temperature). This application note will give a short introduction on power losses and the heat sink, helping to understand the mode of operation and to find the right heat sink for a specific application.

For the thermal design, one needs:

- The maximum power losses $P_{sw,i}$ of each power switch
- The maximum junction temperature $T_{J,max}$ of the power semiconductors
- The junction to ambient thermal resistance impedance $Z_{th,J-A}$. For stationary considerations the static thermal resistance $R_{th,J-A}$ is sufficient. This thermal resistance comprises the junction-to-case thermal resistance $R_{th,J-C}$ as provided in the datasheets, the case to heat sink thermal resistance $R_{th,C-HS}$ accounting for the heat flow through the thermal interface material between heat sink and the power module, and the heat sink-to-ambient thermal resistance $R_{th,HS-A}$. Each thermal resistance can be extended to its corresponding thermal impedance by adding the thermal capacitances.
- The maximum allowed ambient temperature is $T_{A,max}$

Furthermore, all heat flow paths need to be identified. Figure 42 presents a typical simplified equivalent circuit for the thermal network. This circuit is simplified, as it omits thermal capacitance, and typically negligible heat paths such as the heat transfer from the module surface directly to the ambient via convection and radiation.

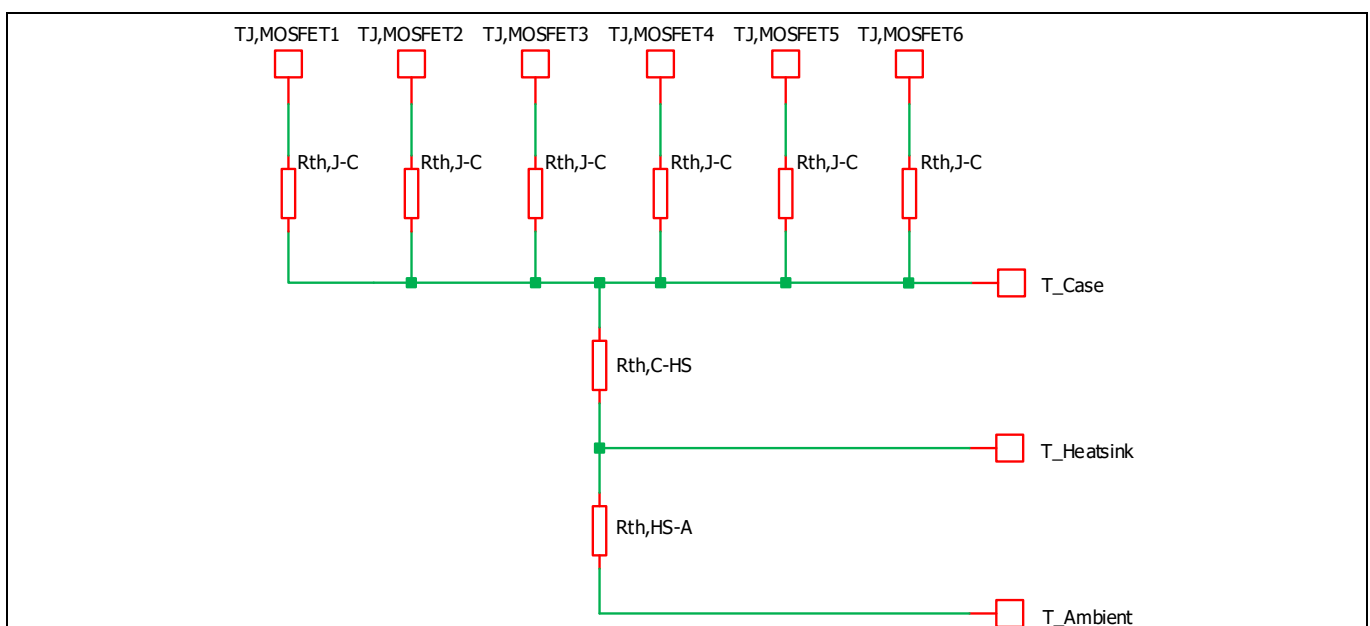


Figure 42 Simplified thermal equivalent circuit

7.2 Power loss

The total power losses in the IM828 are composed of conduction and switching losses in the MOSFETs and body diodes. The loss during the turn-off steady state can be ignored because it is very small and has little effect on increasing the temperature in the device. The conduction loss depends on the DC electrical characteristics of the device, i.e. saturation voltage. Therefore, it is a function of the conduction current and the device's junction temperature. On the other hand, the switching loss is determined by the dynamic characteristics like turn-on/off time and overvoltage/current. Hence, in order to obtain the accurate switching loss, the DC-link voltage of the system, the applied switching frequency and the power circuit layout in addition to the current and temperature should be considered. In this chapter, based on a PWM inverter system for motor control applications, detailed equations are shown to calculate both losses of the IM828 for a 3-phase continuous sinusoidal PWM. For other cases like 3-phase discontinuous PWMs, please refer to [5].

7.2.1 Conduction losses

The typical characteristics of forward drop voltage are approximated by the following linear equation for the IGBT and the diode, respectively.

$$\begin{aligned} V_{\text{IGBT}} &= V_I + R_I \cdot i \\ V_{\text{DIODE}} &= V_D + R_D \cdot i \end{aligned} \quad (6)$$

- V_I = threshold voltage of IGBT
- V_D = threshold voltage of diode
- R_I = on-state slope resistance of IGBT
- R_D = on-state slope resistance of diode

Assuming that the switching frequency is high, the output current of the PWM inverter can be assumed to be sinusoidal. That is,

$$i = I_{\text{peak}} \cos(\theta - \varphi) \quad (7)$$

Where, φ is the phase-angle difference between output voltage and current. Using equations (6) and (7), the conduction loss of one IGBT and its diode can be obtained as follows.

$$P_{\text{con.I}} = \frac{1}{2\pi} \int_0^\pi \xi (V_{\text{IGBT}} \times i) d\theta = \frac{I_{\text{peak}}}{2\pi} V_I + \frac{I_{\text{peak}}}{8} V_I M \cos \varphi + \frac{I_{\text{peak}}^2}{8} R_I + \frac{I_{\text{peak}}^2}{3\pi} R_I M \cos \varphi \quad (8)$$

$$P_{\text{con.D}} = \frac{1}{2\pi} \int_0^\pi (1 - \xi) (V_{\text{DIODE}} \times i) d\theta = \frac{I_{\text{peak}}}{2\pi} V_D - \frac{I_{\text{peak}}}{8} V_D M \cos \varphi + \frac{I_{\text{peak}}^2}{8} R_D - \frac{I_{\text{peak}}^2}{3\pi} R_D M \cos \varphi \quad (9)$$

$$P_{\text{con}} = P_{\text{con.I}} + P_{\text{con.D}} \quad (10)$$

Where ξ is the duty cycle in the given PWM method.

$$\xi = \frac{1 + M \cos \theta}{2} \quad (11)$$

Where, M is the PWM modulation index (M is defined as the peak-phase voltage divided by the half of DC-link voltage).

It should be noted that the total inverter conduction losses are six times the P_{con} .

Thermal system design

7.2.2 Switching losses

Different devices have different switching characteristics, which also vary according to the handled voltage/current and the operating temperature/frequency. However, the turn-on/off loss energy (joule) can be experimentally measured indirectly by multiplying the current and voltage and integrating over time, under a given circumstance. Therefore the linear dependency of the switching energy loss on the switched current is expressed during one switching period as follows.

$$\text{Switching energy loss} = (E_I + E_D) \times i \text{ [joule]} \quad (12)$$

$$E_I = E_{I,ON} + E_{I,OFF} \quad (13)$$

$$E_D = E_{D,ON} + E_{D,OFF} \quad (14)$$

Where, E_I is the switching loss energy of the IGBT and E_D is for its anti-parallel diode. E_I and E_D can be considered approximately as a constant.

As mentioned in the equation (7), the output current can be considered as a sinusoidal waveform; and the switching loss occurs every PWM period for the continuous PWM schemes. Therefore, depending on the switching frequency f_{sw} , the switching loss of one device is represented in the following equation (15).

$$P_{sw} = \frac{1}{2\pi} \int_0^\pi (E_I + E_D) i f_{sw} d\phi = \frac{(E_I + E_D) f_{sw} I_{peak}}{\pi} \quad (15)$$

Where, E_I is a unique constant of IGBT related to the switching energy, and different IGBTs have different E_I values. E_D is one for diode. These should be derived by experimental measurement. From the equation (15), it should be noted that the switching losses are a linear function of current, and directly proportional to the switching frequency.

7.3 Thermal impedance

In practical operation, the power loss P_D is cyclic and therefore the transient impedance needs to be considered. The thermal impedance is typically represented by a RC equivalent circuit (Foster model) as shown in Figure 43. For pulsed power loss, the thermal capacitance effect delays the rise in junction temperature, and thus permits a heavier loading of the IM828. Figure 44 shows thermal impedance from the junction-to-case curves of IM828-XCC. The thermal resistance in Table 25 goes into saturation in about 10 seconds.

Table 25 Thermal resistance of IM828-XCC

Description	Symbol	Condition	Value			Unit
			Min.	Typ.	Max.	
Single-MOSFET thermal resistance, junction-case	R_{thJC}	Low-side U-phase MOSFET (See Figure 4 for T_c measurement point)	-	-	1.45	K/W

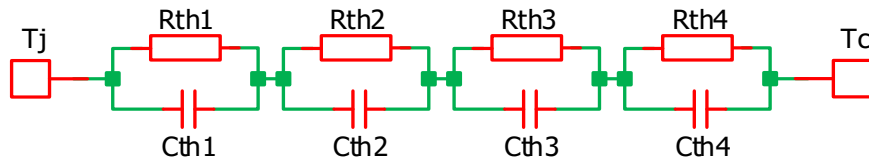


Figure 43 Thermal impedance RC equivalent circuit

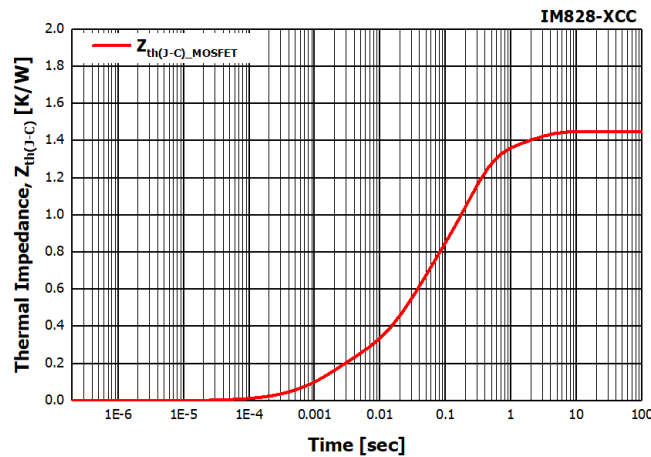


Figure 44 Thermal impedance curves (IM828-XCC based on single-chip heating)

7.4 Temperature rise considerations and calculation example

The IPM 3-phase inverter simulator [6] based on PLECS allows users to calculate power losses and temperature profiles with three heat sink mounting options (Mounted heat sink, in free air, fixed reference). The result of loss & temperature calculation using the typical characteristics is shown in Figure 45 as simulation example (for $V_{PN} = 600\text{ V}$, $V_{DD} = 15\text{ V}$, $V_{DS(ON)} = \text{typical}$, switching losses = typical, $T_J = 150^\circ\text{C}$, $F_{SW} = 20\text{ kHz}$, $R_{th(J-C)} = \text{Max.}$, P.F = 0.99, MI = 0.60, $I_o = 14.14\text{ A}_{rms}$, $T_C = 100^\circ\text{C}$ (fixed reference), SVPWM modulation, 60 Hz sine waveform output).

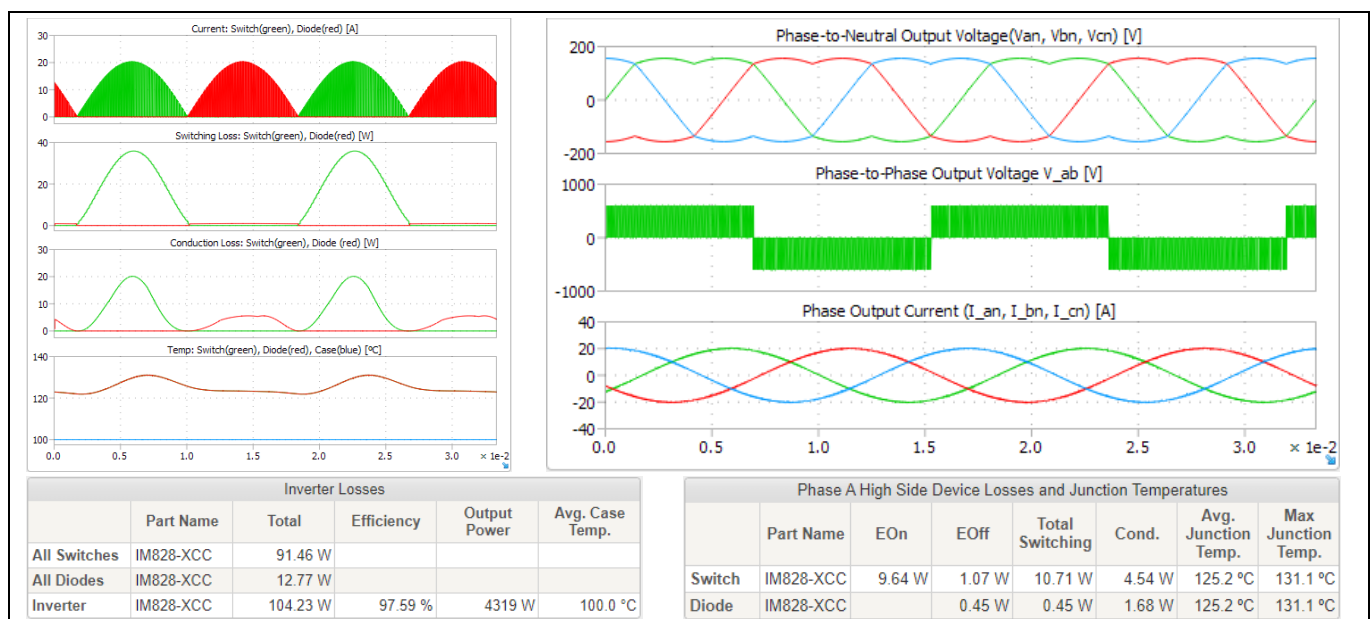


Figure 45 IPM 3-phase inverter simulation results of IM828-XCC [6]

7.5 Heat sink selection guide

7.5.1 Required heat sink performance

If the power losses $P_{sw,i}$, $R_{th(J-C)}$ and the maximum ambient temperature are known, the required thermal resistance of the heat sink and the thermal interface material can be calculated according to 0 from,

$$T_{J,max} = T_{A,max} + \sum_i P_{sw,i} \cdot R_{th,HS-A} + \sum_i P_{sw,i} \cdot R_{th,C-HS} + \text{Max}(P_{sw,i} \cdot R_{th,JC,i}) \quad (16)$$

For three- phase bridges, one can simply assume that all power switches dissipate the same power and all have the same $R_{th,J-C}$. This leads to the required thermal resistance from case to ambient.

$$R_{th,C-A} = R_{th,C-HS} + R_{th,HS-A} = \frac{T_{J,max} - P_{sw} \cdot R_{th,JC} - T_{A,max}}{\sum P_{sw}} \quad (17)$$

For example, the power switches of a washing machine drive dissipate 3.5 W maximum each, the maximum ambient temperature is 50°C, the maximum junction temperature is 150°C and $R_{th(J-C)}$ is 3 K/W. It results in:

$$R_{th,C-A} \leq \frac{150^{\circ}\text{C} - 3.5\text{W} \cdot 3 \frac{\text{K}}{\text{W}} - 50^{\circ}\text{C}}{6 \cdot 3.5\text{W}} = 4.3 \frac{\text{K}}{\text{W}}$$

If the heat sink temperature shall be limited to 100°C, an even lower thermal resistance is required:

$$R_{th,C-A} \leq \frac{100^{\circ}\text{C} - 50^{\circ}\text{C}}{6 \cdot 3.5\text{W}} = 2.4 \frac{\text{K}}{\text{W}}$$

Smaller heat sinks with higher thermal resistance may be acceptable if the maximum power is only required for a short time (times below the time constant of the thermal resistance and the thermal capacitance). However, this requires a detailed analysis of the transient power and temperature profiles. The larger the heat sink, the larger the thermal capacitance and the longer it takes to heat up the heat sink.

7.5.2 Heat sink characteristics

Heat sinks are characterized by three parameters:

- Heat transfer from the power source to heat sink
- Heat transfer within the heat sink (to all the surfaces of the heat sink)
- Heat transfer from heat sink surfaces to ambient

7.5.2.1 Heat transfer from heat source to heat sink

There are two factors which need to be considered in order to provide a good thermal contact between power source and heat sink:

- **Flatness of the contact area**

Due to the unevenness of surfaces, a thermal interface material needs to be supplied between heat source and heat sink. However, such materials have a rather low thermal conductivity ($< 10 \text{ K/W}$). Hence these materials should be as thin as possible. On the other hand, they need to fill out the space between heat source and heat sink. Therefore, the unevenness of the heat sink should be as low as possible. In addition, the particle size of the interface material must fit to the roughness of the module and the heat sink surfaces. Particles that are too large will unnecessarily increase the thickness of the interface layer, and hence increase the thermal resistance. Particles that are too small will not provide a good contact between the two surfaces and will lead to a higher thermal resistance as well.

- **Mounting pressure**

The higher the mounting pressure, the better the interface material disperses. Also excessive interface material is squeezed out resulting in a thinner interface layer with a lower thermal resistance.

7.5.2.2 Heat transfer within the heat sink

The heat transfer within the heat sink is mainly determined by:

- **Heat sink material**

The material needs to be a good thermal conductor. Most heat sinks are made of aluminum ($\lambda \approx 200 \text{ W/(m}^*\text{K)}$). Copper is heavier and more expensive but also nearly twice as efficient ($\lambda \approx 400 \text{ W/(m}^*\text{K)}$).

- **Fin thickness**

If the fins are too thin, the thermal resistance from heat source to fin is too high, and the efficiency of the fin decreases. Hence it does not make sense to make the fins as thin as possible in order to make more fins and therefore to increase the surface area.

7.5.2.3 Heat transfer from heat sink surface to ambient

The heat transfers to the ambient mainly by convection. The corresponding thermal resistance is defined as

$$R_{\text{th,conv}} = \frac{1}{\alpha \cdot A} \quad (18)$$

Where α is the heat transfer coefficient and A is the surface area.

Hence there are two important parameters:

- **Surface area:** Heat sinks require a huge surface area in order to easily transfer the heat to the ambient. However, as the heat source is assumed to be concentrated at one point and not uniformly distributed, the total thermal resistance of a heat sink does not change linearly with length. Also, increasing the surface area by increasing the number of fins does not necessarily reduce the thermal resistance as discussed in Section 7.5.2.2.
- **Heat transfer coefficient (aerodynamics):** This coefficient strongly depends on the air flow velocity as shown in Figure 46. If there is no externally induced flow, one speaks of natural convection. Otherwise it is forced convection. Heat sinks with very small fin spacing do not allow a good air flow. If a fan is used, the fin gap may be lower than for natural convection, as the fan forces the air through the space between the fins.

Thermal system design

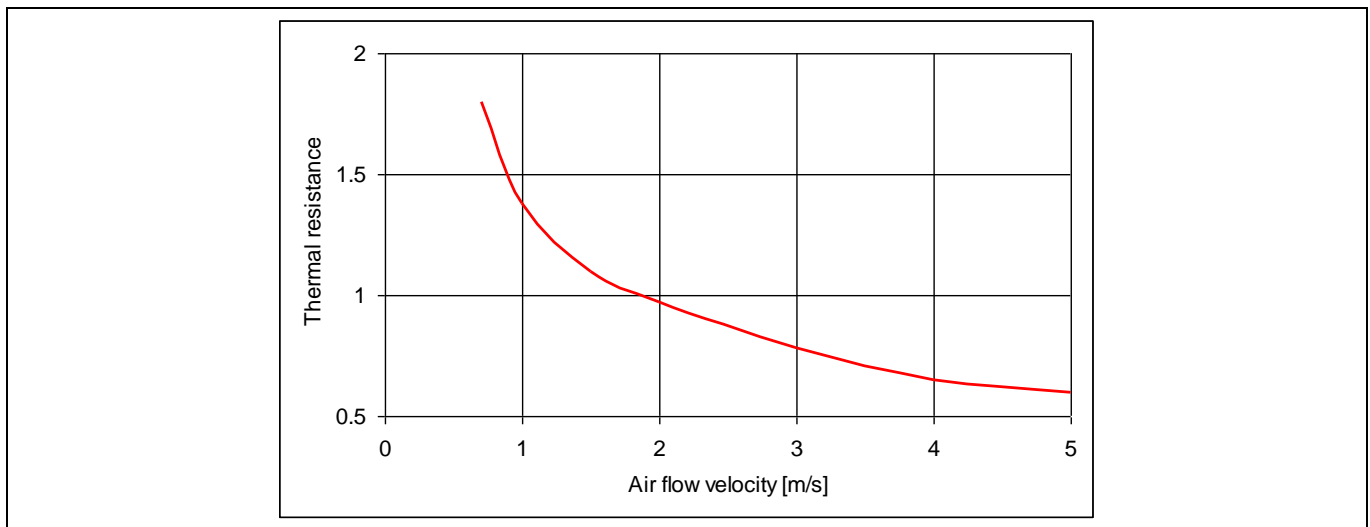


Figure 46 Thermal resistance as a function of the air flow velocity

Furthermore, in the case of natural convection, the heat sink efficiency depends on the temperature difference of heat sink and ambient, i.e. on the dissipated power. Some manufacturers, like Aavid Thermalloy, provide a correction table which allows the user to calculate the thermal resistance depending on the temperature difference. Figure 47 shows the heat sink efficiency degradation for natural convection as provided in [7]. Please note that the thermal resistance is 25% higher at 30 W than at 75 W.

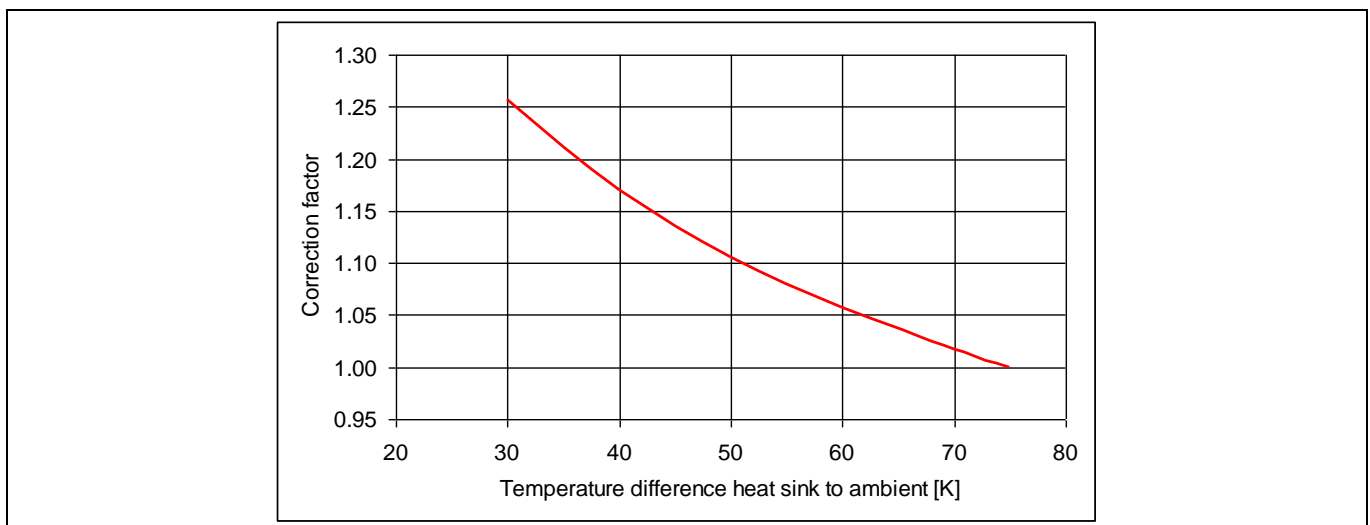


Figure 47 Correction factors for temperature

The positioning of the heat sink also plays an important role in the aerodynamics. In the case of natural convection, the best mounting is done with vertical fins, as the heated air tends to move upwards due to buoyancy. Furthermore, one should make sure that there are no significant obstructions impeding the air flow.

Radiation occurs as well supporting the heat transfer from heat sink to ambient. In order to increase radiated heat, one can use anodized heat sinks with a black surface. However, this decreases the thermal resistance of the heat sink only by a few percentage points in the case of natural convection. Radiated heat is negligible in the case of forced convection. Hence blank heat sinks can be used if no fan is used with the heat sink.

The discussions in this section clearly show that there cannot be a single thermal resistance value assigned to a certain heat sink.

7.5.3 Selecting a heat sink

Unfortunately, there are no straightforward formulas for selecting heat sinks. Finding an appropriate heat sink will include an iterative process of choosing and testing heat sinks. In order to get a first rough estimation of the required volume of the heat sink, one can start with estimated volumetric thermal resistances as given in Table 26 (taken from [8]). This table gives only a first clue, as the actual resistance may vary depending on many parameters like actual dimensions, type and orientation, etc.

Table 26 Volumetric thermal resistance

Flow conditions [m/s]	Volumetric resistance [cm ³ °C/W]
Natural convection	500 ~ 800
1.0	150 ~ 250
2.5	80 ~ 150
5.0	50 ~ 80

One can roughly assume that the volume of a heat sink needs to be quadrupled in order to halve its thermal resistance. This gives a hint whether natural convection is sufficient for the available space, or whether forced convection is required.

In order to get an optimized heat sink for a given application, one needs to contact heat sink manufacturers or consultants. Further hints and references can be found in [7].

When contacting heat sink manufacturers in order to find a suitable heat sink, please note the conditions under which the given thermal resistance values are valid. They might be given either for a point source or for a heat source which is evenly distributed over the entire base area of the heat sink. Also take care that the fin spacing is optimized for the corresponding flow conditions.

8 Heat sink mounting and handling guidelines

8.1 Electrical spacing

The electric spacing specifications of IM828 are shown in Table 27. The IM828 package(DIP 36X23D) does not satisfy the clearance and creepage distance between pins and heat sink (earthed) and the creepage distance on the PCB between signal pins such as (2) to (3), (4) to (5), (6) to (7). Based on IEC and UL standards, to secure a clearance and creepage distance between the pins and the heat sink (earthed), a convex-shaped heat sink is necessary as shown in Figure 48, and the PCB slot is required to keep 4.0 mm creepage on the PCB between the signal pins.

Table 27 Electrical spacing (*not compliant to IEC)

Standard & CIPOS™ Maxi	IPM Unit				PCB		Remark
	Basic insulation pin to heat sink(earthed) [mm]		Functional insulation between pin and pin [mm]		PWB (solder to solder) [mm]		
	Clearance	Creepage	Clearance	Creepage	Clearance	Creepage	
IEC60335-1 IEC60664-1 IEC67800-5-1 UL840	5.5	4.0	3.0	4.0	3.0	4.0	Refer to Table 21
CIPOS™ Maxi IM828 IPM	*1.6	*1.62	Power pins: 4.97 Signal pins: 3.33	Power pins: 5.17 Signal pins: 4.12	Power pins: 4.94 Signal pins: 3.53	Power pins: 4.94 Signal pins: *3.53	PCB slot is necessary.

Table 28 Boundary conditions

Isolation	Rated voltage	Overvoltage category	Impulse voltage	Working voltage	Working voltage	Pollution degree	IPM CTI
Pin to heat sink (earthed)	480 V _{ac}	III	6000 V	679 V _{dc}	Max. 800 V _{dc}	II	> 600
Pin to pin	480 V _{ac}	II	4000 V	679 V _{dc}	Max. 800 V _{dc}	II	> 600

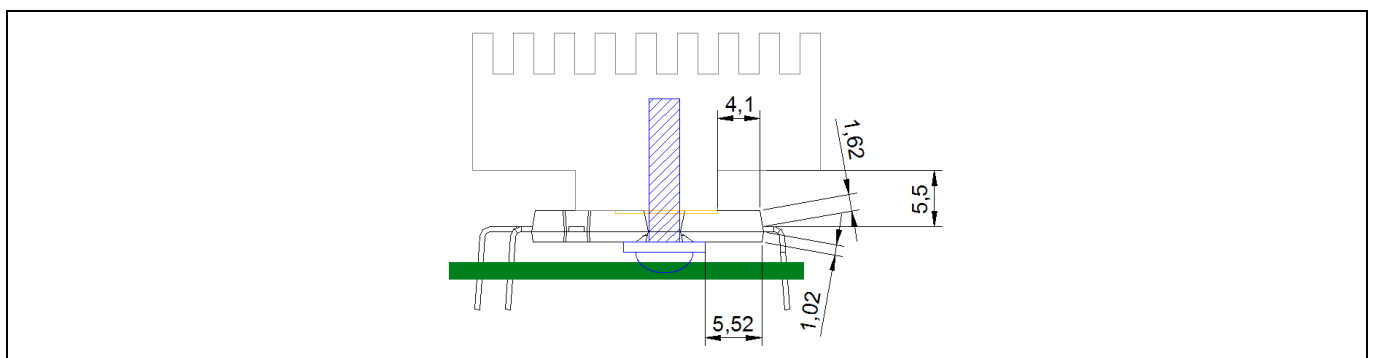


Figure 48 Recommended heat sink shape to get creepage and clearance distance between pins and heat sink (Dimension is symmetric)

8.2 Heat sink mounting

8.2.1 General guidelines

An adequate heat-sinking capability of the IPM is only achievable if the heat sink is suitably mounted. This is the fundamental requirement in order to meet the electrical and thermal performance criteria of the module. The following general points should be observed when mounting the IPM on a heat sink. Verify the following points related to the heat sink:

- a) There must be no burrs on aluminum or copper heat sinks.
- b) Screw holes must be countersunk.
- c) There must be no unevenness or scratches in the heat sink.
- d) The surface of the module must be completely in contact with the heat sink.
- e) There must be no oxidation, stain or burrs on the heat sink surface.

To improve the thermal conductivity, apply silicone grease to the contact surface between the IPM and heat sink. Spread a homogenous layer of silicone grease with a thickness of 100 µm over the IPM substrate surface. Non-planar surfaces of the heat sink may require a thicker layer of thermal grease. Please refer here to the specifications of the heat sink manufacturer. It is important to note here that the heat sink covers the complete backside of the module. There may be different functional behavior if there is a portion of the backside of the module which is not in contact with the heat sink.

To prevent a loss of heat dissipation effect due to warping of the substrate, tighten down the mounting screws gradually and sequentially while maintaining a left/right balance in pressure applied.

It must be assured by design of the application PCB, that the plane of the back side of the module and the plane of the heat sink are parallel in order to achieve minimal tension of the package and an optimal contact of the module with the heat sink. Please refer to the mechanical specifications of the module given in the datasheets.

It is the basics of good engineering to verify the function and thermal conditions by means of detailed measurements. It is best to use a final application inverter system, which is assembled with the final production process. This helps to achieve high-quality applications.

8.2.1.1 Recommended tightening torque

As shown in Table 29, the tightening torque of M3 screws is specified for a minimum $MS = 0.49 \text{ N}\cdot\text{m}$ and a maximum $MS = 0.78 \text{ N}\cdot\text{m}$. The screw holes must be centered to the screw openings of the mold compound, so that the screws do not contact the mold compound. If an insulating sheet is used, use a sheet larger than the IPM, which should be aligned accurately when attached. It is important to ensure that no air is enclosed by the insulating sheet. Generally speaking, insulating sheets are used in the following cases:

- When the ability of withstanding primary and secondary voltages is required to achieve required safety standard against a hazardous situation.
- When the IM828 must be insulated from the heat sink.
- When measuring the module, to reduce radiated noise or eliminate other signal-related problems.

Table 29 Mechanical characteristics and ratings

Item	Condition	Value			Unit
		Min.	Typ.	Max.	
Mounting torque	Mounting screw : M3	0.49	-	0.78	N·m
Backside curvature	(Note Figure 49)	0	-	+150	μm
Heat sink flatness	(Note Figure 50)	0	-	+100	μm
Weight		-	7.1	-	g

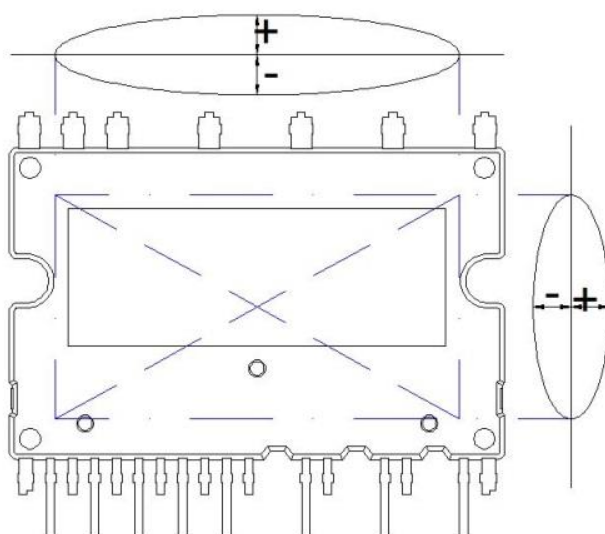


Figure 49 Backside curvature measurement position

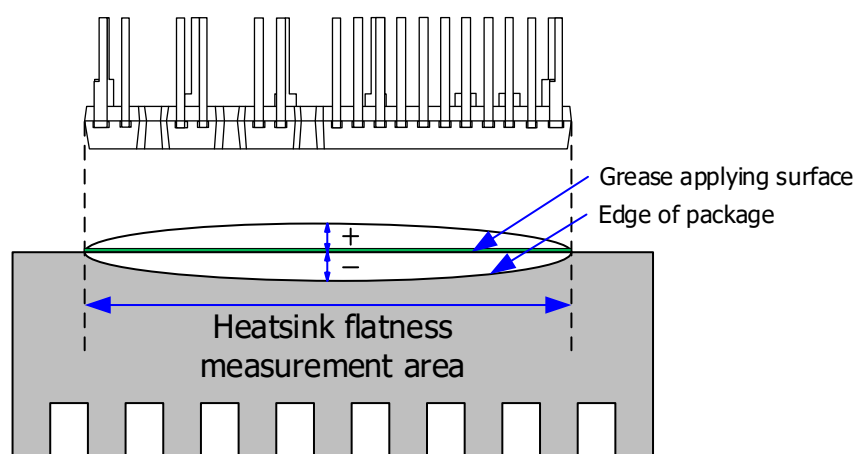


Figure 50 Heat sink flatness measurement position

8.2.1.2 Screw-tightening to heat sink

The tightening of the screws is the main process of attaching the module to the heat sink. It is assumed that an interface pad is attached to the heat sink surface, which extends to the edge of the module and is located for the fixing holes. It is recommended that M3 fixing screws are used in conjunction with a spring washer and a plain washer. The spring washer must be assembled between the plain washer and the screw head. The screw torque must be monitored by the fixing tool.

Tightening process:

- Align module with the fixing holes.
- Insert screw A with washers to touch only position (pre-screwing).
- Insert screw B with washers (pre-screwing).
- Tighten screw A to final torque.
- Tighten screw B to final torque.

Note: The pre-screwing torque is set to 20~30% of maximum torque rating.

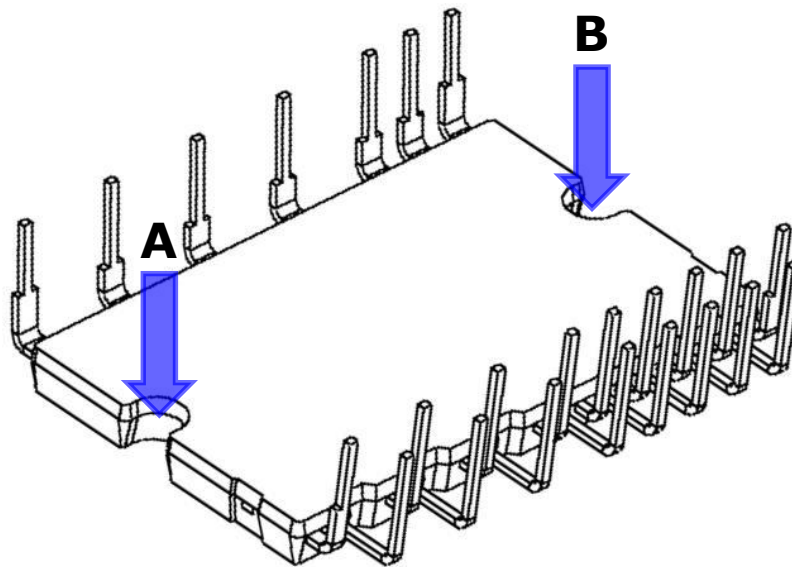


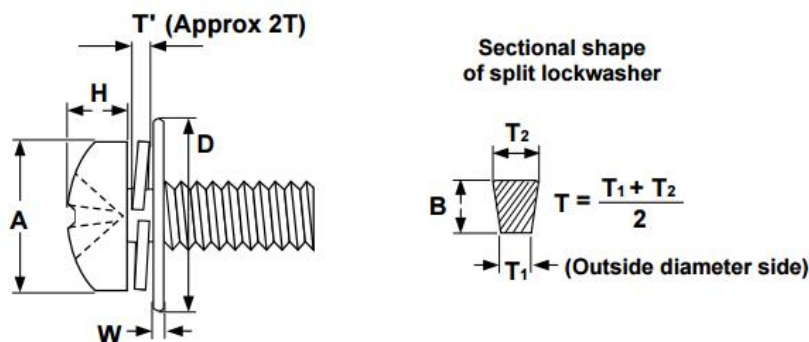
Figure 51 Recommended screw-tightening order : Pre-screwing A → B, Final screwing A → B

8.2.1.3 Mounting screw

When we attach module to heat sink, we recommend M3 SEMS screws (JIS B1256/JIS B1188) as shown in Table 30.

Table 30 Recommended screw specifications (Typical)

Screw dimensions				Flat washer		Spring washer	
Size	Thread pitch	A	H	D	W	D1	B x T
		Head diameter	Head height	Outer diameter	Thickness	Outside diameter	
M3	0.5	5.2	2.0	7.8	0.58	5	1.1 x 0.7



8.2.2 Recommended heat sink shape and mechanical assembly

A shock or vibration through the PCB or heat sink might cause the crack of the package mounted on the heat sink. To avoid a broken or cracked package and to endure shock or vibration through PCB or heat sink, a heat sink shape is recommended as shown in Figure 52. The heat sink needs to be fixed to the PCB with screws or eyelets. In the mass-production stage, the process sequence for system assembly in terms of device soldering on PCB, heat sink mounting and casing etc., should be taken into account to avoid mechanical stress on the device pins, package mold compound, heat sink and system enclosure, etc.

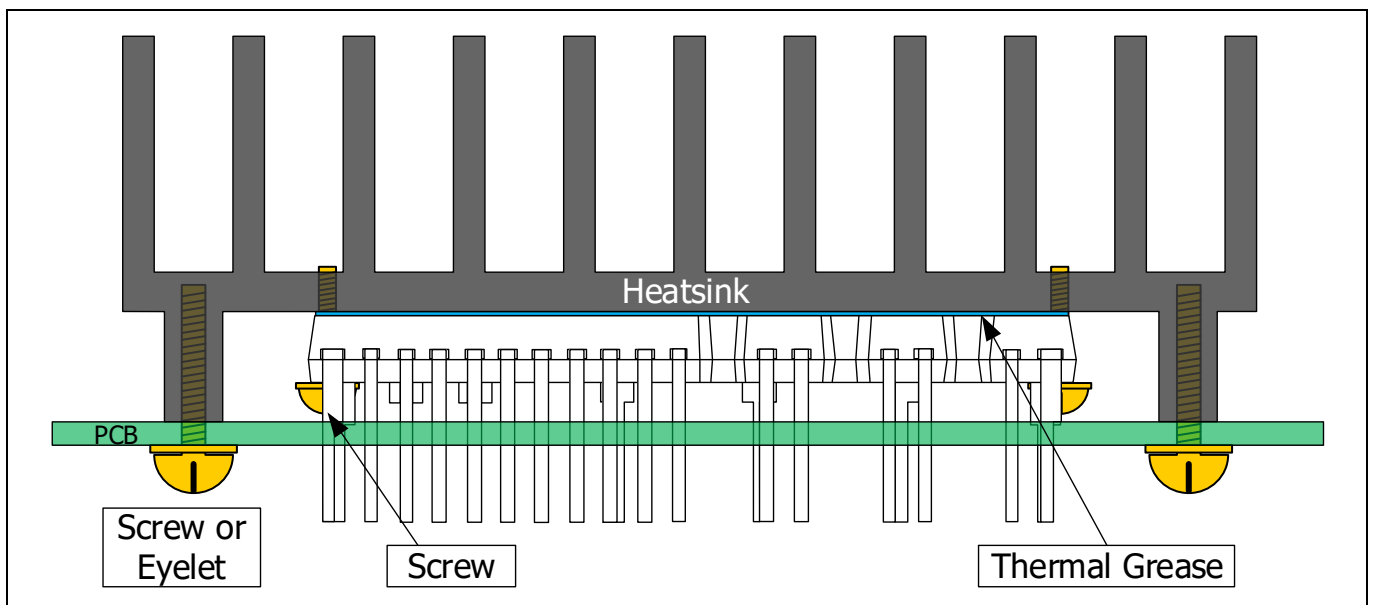


Figure 52 Recommended heat sink shape

8.3 Handling guidelines

When installing a module to a heat sink, excessive uneven tightening force might apply stress to inside chips, which will lead to breaking or degradation of the device. An example of recommended fastening order is shown in Figure 51.

- Do not over-torque when mounting the screws. Excessive mounting torque may cause damage to module holes as well as to the screws and heat sink.
- Avoid one-side tightening stress. Uneven mounting can cause the module holes to be damaged.

To get effective heat dissipation, it is necessary to enlarge the contact area as much as possible, which minimizes the contact thermal resistance.

Properly apply thermal conductive grease over the contact surface between the module and the heat sink, which is also useful for preventing the contact surface from corrosion. Furthermore, the grease should be of stable quality and long-term durability within a wide operating-temperature range. Use a torque wrench to tighten to the specified torque rating. Exceeding the maximum torque limitation might cause a module to be damaged or degraded. Make sure there is no dirt remaining on the contact surface between the module and the heat sink. All equipment used to handle or mount the IPM must comply with the relevant ESD standards. This includes transportation, storage and assembly. The module itself is an ESD-sensitive device. It may therefore be damaged in case of ESD shocks.

Do not shake or grasp the heat sink; in particular, avoid any chocks to the PCB by grasping only the heat sink. This could cause package cracking or breaking.

8.4 Storage guidelines

8.4.1 Recommended storage conditions

Temperature: 5 ~ 35 °C

Relative humidity: 45 ~ 75%

- Avoid leaving the IM828 exposed to moisture or direct sunlight. In particular be careful during periods of rain or snow.
- Use storage areas where there is minimal temperature fluctuation.

Rapid temperature changes can cause moisture condensation on the stored IM828-XCC, resulting in lead oxidation or corrosion as a result, leading to degraded solderability.

- Do not allow the IM828-XCC to be exposed to corrosive gasses or dusty conditions.
- Do not allow excessive external forces or loads to be applied to the IM828-XCC while they are in storage.

References

9 References

1. D. Peters et.al: The new CoolSiC™ Trench MOSFET Technology for Low Gate Oxide Stress and High Performance, May 2017, Proc. PCIM 2017, Nuremberg
2. AN2017-46 CoolSiC™ 1200V SiC MOSFET application note, Infineon Technologies
3. R. Keggenhoff, Z.Liang, Andre Arens, P. Kanschat, R. Rudolf. 'Novel SOI Driver for Low Power Drive Applications', Power Systems Design Europe Nov. 2005
4. M. Lee, M. Baek, J. Lee, D. Chung "A New Smallest 1200V Intelligent Power Module for Three Phase Motor Drives", IPEC 2018, Niigata, Japan
5. D. Chung, S. Sul, "Minimum-Loss Strategy for three-Phase PWM Rectifier", IEEE Transactions on Industrial Electronics, Vol. 46, No. 3, June, 1999
6. IPM 3-Phase Inverter Simulator, <https://plex.infineon.com/plexim/ipmmotor.html>
7. Aavid Thermalloy, <http://www.aavidthermalloy.com/technical/correct.shtml>
8. S. Lee, "How to select a heat sink", Electronics Coolings, Vol.1, No.1, June 1995
9. AN2018-09 Guideline for CoolSiC MOSFET gate drive voltage window, Infineon Technologies

References

Revision History

Major changes since the last revision

Version Number	Revision date	Description of change
1.00	2020-09-22	Initial release
1.01	2021-09-06	Changed Figure 5. Corrected data in Table 27. (Clearance for signal pin: 4.12mm → 3.33mm)

Trademarks

All referenced product or service names and trademarks are the property of their respective owners.

Edition 2021-09-06

Published by

Infineon Technologies AG

81726 Munich, Germany

© 2021 Infineon Technologies AG.

All Rights Reserved.

Do you have a question about this document?

Email: erratum@infineon.com

Document reference

AN2020-41

IMPORTANT NOTICE

The information contained in this application note is given as a hint for the implementation of the product only and shall in no event be regarded as a description or warranty of a certain functionality, condition or quality of the product. Before implementation of the product, the recipient of this application note must verify any function and other technical information given herein in the real application. Infineon Technologies hereby disclaims any and all warranties and liabilities of any kind (including without limitation warranties of non-infringement of intellectual property rights of any third party) with respect to any and all information given in this application note.

The data contained in this document is exclusively intended for technically trained staff. It is the responsibility of customer's technical departments to evaluate the suitability of the product for the intended application and the completeness of the product information given in this document with respect to such application.

For further information on the product, technology delivery terms and conditions and prices please contact your nearest Infineon Technologies office (www.infineon.com).

Please note that this product is not qualified according to the AEC Q100 or AEC Q101 documents of the Automotive Electronics Council.

WARNINGS

Due to technical requirements products may contain dangerous substances. For information on the types in question please contact your nearest Infineon Technologies office.

Except as otherwise explicitly approved by Infineon Technologies in a written document signed by authorized representatives of Infineon Technologies, Infineon Technologies' products may not be used in any applications where a failure of the product or any consequences of the use thereof can reasonably be expected to result in personal injury.